CHALMERS

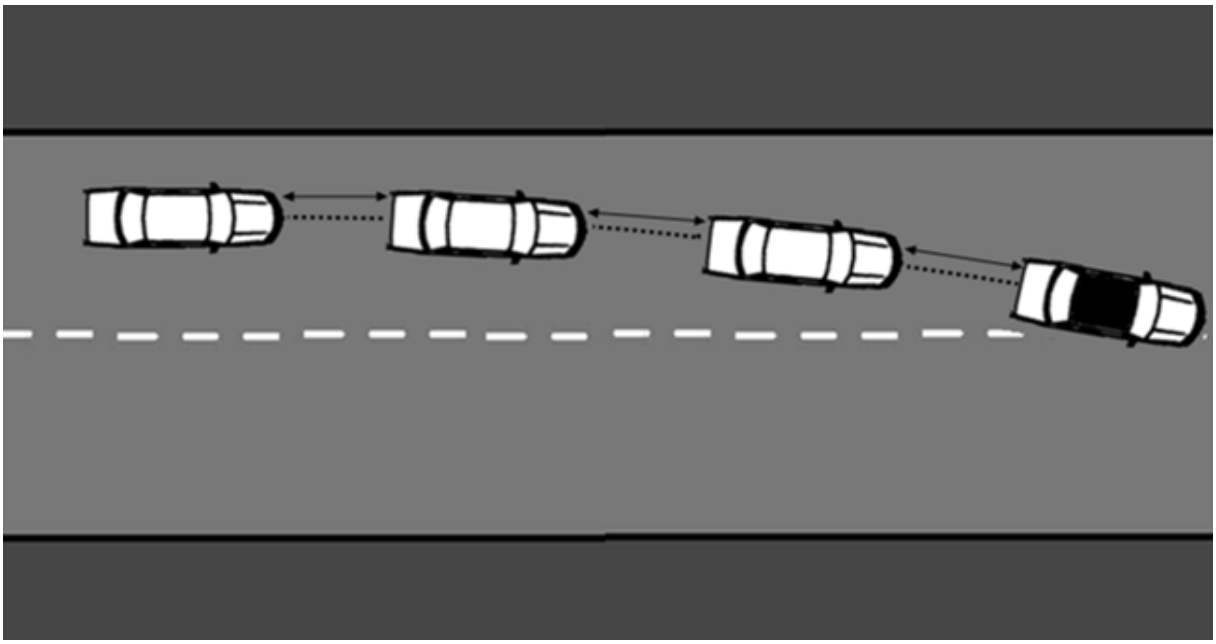

Lateral Control of Vehicle Platoons

Master's Thesis in Systems, Control and Mechatronics

ARASH IDELCHI

BADR BIN SALAMAH

Department of Signals and Systems
Division of Automatic Control, Automation and Mechatronics
CHALMERS UNIVERSITY OF TECHNOLOGY
Göteborg, Sweden, 2011

Report No. EX053/2011

Lateral Control of Vehicle Platoons

Arash Idelchi
Badr Bin Salamah

Report No. EX053/2011
Department of Signals and Systems
Division of Automatic Control, Automation and Mechatronics
Chalmers University of Technology
Göteborg, 2011

SE-412 96 Göteborg
Sweden
Telephone: +46 (0)31-7721000

ABSTRACT

The notion of vehicles moving in platoons is of considerable interest when seeking to decrease traffic congestion and gas consumption. This usually means automated operation in longitudinal and possibly lateral direction. This report focuses on the lateral dynamics and control of a vehicle platoon following a leader in the lateral direction. A thorough system modelling and analysis is conducted and different classical control approaches discussed. It is noted that overshoot cannot be avoided in the system when using reasonable feedback controllers, due to the inherent characteristics of the plant. The concept of string stability (i.e damping the propagation of errors in the platoon) is covered along with different communication topologies, which under certain assumptions will guarantee stability. It is noted that solely communicating the preceding vehicle's lateral error will not result in string stability. A novel compensation is introduced taking into account information from several vehicles, which is proven to give a string stable system.

Key words: Lateral vehicle control, Vehicle platoon, String stability, Vehicle following

ACKNOWLEDGEMENTS

We would like to extend our thanks firstly and most importantly to our supervisor Stefan Solyom, whose excellent guidance has helped shape this project. Furthermore, we would like to thank Professor Bo Egardt, for interesting discussions and inputs. We would also like to thank VCC for making this thesis possible and for supplying us with the resources and tools we needed to complete this project.

Lastly, we'd like to thank our friends and families for their support during this time.

CONTENTS

List of Figures

List of Symbols

ψ	Yaw rate
V_x	Longitudinal velocity
$\boldsymbol{V}$	Velocity vector
β	Slip angle
y	Lateral position
m	Mass
a_y	Inertial acceleration
F_{yf}	Front wheel force
F_{yr}	Rear wheel force
I_z	Moment of inertia
l_f	Length to front wheels
l_r	Length to rear wheels
δ	Steering wheel angle
θ_{Vf}	Front wheel angle to velocity vector
θ_{Vr}	Rear wheel angle to velocity vector
α_f	Front wheel slip angle
α_r	Rear wheel slip angle
$C_{\alpha f}$	Stiffness coefficient for front wheels
$C_{\alpha r}$	Stiffness coefficient for rear wheels
C_f	Stiffness coefficient for front wheel
C_r	Stiffness coefficient for rear wheel
Δy	Lateral deviation
Y_L	Projected lateral distance
Y_T	Leading vehicle's lateral distance
Y_F	Following vehicle's lateral distance
l_{rb}	Length to front bumper
τ	Time constant
K_p	Proportional gain
K_i	Integral gain
H_i	Arbitrary transfer function
γ	L_2-induced gain
K_d	Derivative gain
T_d	Derivative time
T_f	Filter time constant
ε	Lateral error measure (frequency plane)
$y_e^{(i)}$	Lateral error (time plane)
F	Feedforward filter
C	Controller

1 Introduction

This chapter will give a brief overview of the project, topics discussed, as well as goals and limitations.

1.1 Background

The concept of having a vehicle platoon moving in unison, whether in longitudinal or lateral direction, is of considerable interest when seeking to decrease traffic congestion and gas consumption, improve driver comfort and safety, and limit emissions [1] [2]. In the platoon, the objective to achieve, for the longitudinal case, is each vehicle maintaining a safe and predetermined distance to the vehicle in front, called the leader. The distance would typically be dependant of velocity, since higher velocities require larger safety-distances [2].The driver thus lets the gas and brake of the vehicle be handled automatically. In the lateral case, the objective is to, in a stable manner, follow the path of the leading vehicle and mimic its manoeuvres using a control algorithm. The driver can then hand over the steering to the computer.

However, much research has been focused on utilization of vehicle platoons operating in specialized infrastructure, such as highways with magnets integrated into the path and used as road markings [2]. Recent developments are more tended toward the implementation of platoons in unmodified roads using available sensor information and communication, such as angle and distance to preceding car, to determine acceleration, braking or steering [3].

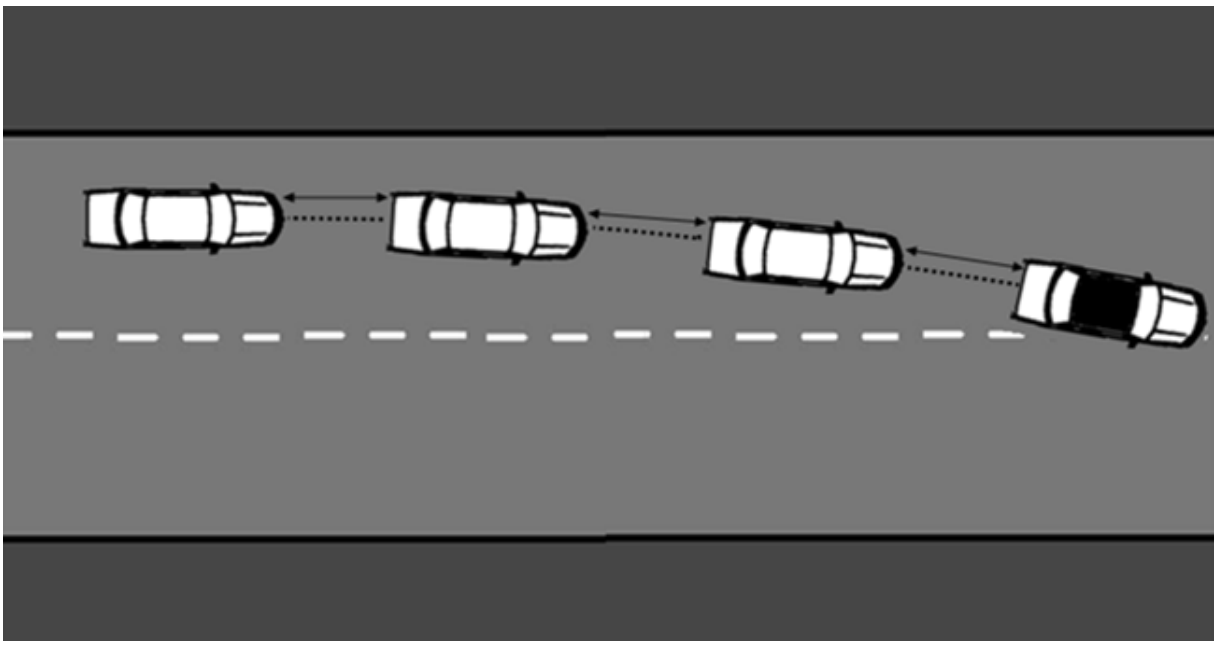

Figure 1.1.1: Depiction of a platoon performing a lane-change with the leader marked black.

The picture above illustrates the concept; each vehicle will depending on its state and the state of the neighbouring vehicle utilize a control strategy to follow its movements and maintain the platoon. The platoon can under these assumptions be seen as decentralized. A serious issue that may arise here is error propagation throughout the platoon. In the case of the first

following car being laterally displaced relative to the leader, the displacement might be amplified to the second follower, and so on. This problem needs to be either eradicated or bounded, i.e string stability has to hold, to avoid vehicles further down the line leaving the lane. Communication between vehicles, provided the delay is short enough, play an important role in dealing with this problem. Thus there are two important points when dealing with automated platoons; a control strategy that ensures string stability, and the assumptions or infrastructures necessary to implement these.

Previous work has been much focused on vehicle platoons in which lane-keeping or tracking has been involved, and thus not clearly described the difficulties to attain string stability in vehicle-following systems. However, all conclude the fact that there is some need of communication strategies to assure string stability.

1.2 Purpose and Aims

The main focus of this thesis was to design a controller which stabilizes a system of vehicles following in the lateral direction, provides adequate response and finally guarantees or enforces string stability under certain assumptions. For this to be achieved, literature studies were required, proper understanding of the vehicle model, system and various controller design techniques. Thus, the report is segmented into several parts; theory of vehicle dynamics, modelling of the vehicle, modelling and analysis of a two-vehicle following system, controller design approaches, and finally testing and verification theoretically in a software environment as well as implementation in vehicles at Volvo Car Corporation.

The whole problem can be partitioned into two main parts;

1) The *regulation problem*, consisting of obtaining a controller design and communication topology that would stabilize the system and yield some criteria for string stability.

2) The *path-following problem*, in which a suitable reference-signal to each individual in the platoon should be determined to satisfy proper following.

Of these two parts, the former will be given most attention in this report, while the latter will be touched upon briefly in the discussion.

1.3 Methodology

To accomplish the goals mentioned above, extensive research in the areas of vehicle dynamics and control was required. This was conducted through the study of relevant papers published in the field as well as literature studies. The system was thereafter modelled, partitioned analytically and analyzed in terms of characteristics such as frequency domain behaviour and stability. Several controller techniques were utilized and the performance of each was systematically evaluated in MATLAB, while simulations of basic vehicle following were carried out in Simulink. The controllers were finally implemented on vehicles at Volvo Car Corporation.

1.4 Scope and Limitations

Initially, the research was restricted to the modelling of a two-car system and development of a controller which performs according to specifications. To enable simpler analysis, the vehicle model was linearized and only linear controllers were considered. The algorithm was then evaluated on a larger sized platoon to verify robustness and restrictions on the use of the algorithm depending on the number of cars in the platoon. The sensor information available was assumed to be a wide range of vision and radar information; such as angle and distance between each vehicle, while communication relays steering-wheel angle, velocity as well as partial state information throughout the platoon. Furthermore, the maximum amount of lag that may be present in the system was assumed to be 100ms, while the actuator of the steering-wheel was approximated by a first-order lag with a time-constant. The platoon considered consists of identical vehicles, where all vehicle-related parameters were assumed non-varying with the exception of velocity and look-ahead distance. Finally, no manoeuvres inducing offsets of larger than 15 degrees between each vehicle were considered.

2 Preliminaries

This chapter will briefly discuss simple terms and concepts that will facilitate understanding for the reader.

2.1 Look-Ahead Distance

The term *look-ahead* denotes in vehicle applications the concept of communicating the position of a point at a certain distance (referred to as the *look-ahead distance*) to the vehicle. To reach this goal different techniques can be used; for example through GPS or attaching a sensor on the front of the vehicle to monitor the relative position of the preceding vehicle's rear bumper.

This technique is in sharp contrast to the so called *lane-keeping* or *look-down* methods, since its implementation in a platoon will lead to an interconnected system, while the latter enable each vehicle to track the reference line independently of the performance of preceding or following vehicles. Hence, there is no need for stability analysis for the platoon; however the amount of infrastructure needed (such as magnets positioned on the lanes or road-marker cameras) and dedicated highways required for this system becomes an issue.

The look-ahead distance has strong effect on the stability and performance of the closed loop system; it was shown in [4] that closed loop stability can always be achieved for a constant proportional control law by increasing the look-ahead distance to an appropriate value. The impact on the damping of the system caused by variations in the look-ahead distance will be clearly discussed in Section 4.

2.2 Sensors and Inter-Vehicle Communication

The sensor information used to determine lateral offset to the preceding vehicle is obtained from a camera, radar, and laser mounted on the windshield of the vehicle. By measuring the distance and angle to a fixed point on the preceding vehicle's bumper, a suitable approximation can be made. Inter-vehicle communication is present in the system as well; measurements of yaw-rate, steering-wheel angle and velocity are available to convey throughout the platoon with negligible delay assumed.

3 Modelling

This chapter is divided into two parts; the former deals with theory behind a basic linear vehicle model while the latter forms the equations needed for analysis of a vehicle-following system.

3.1 Vehicle Model

The lateral motion of a front-wheel driven vehicle can be modelled mathematically using kinematics, where the equations of models are simply geometric relationships within the system. However, this approach is only suitable for low velocities (speeds less than 5m/s) since it is assumed that the velocity-vector at each wheel is in the direction of the wheel-angle; in other words, there is no *slip* at the wheels, and the slip-angle is hence zero [1].

Since this project focuses on tight platoons of relatively high speeds (i.e. above 5m/s) this assumption no longer holds and a dynamic model taking the slip-angle into consideration has to be developed.

The model used is a linear, so-called *bicycle model*, where the two front wheels have been merged and represented as one single wheel, with the two rear wheels also treated similarly. This will simplify the modelling process is deemed to be satisfactory for analysis.

Consider the figure below, showing a bicycle model of the vehicle and its orientation with respect to some global coordinate-system ($\boldsymbol{X}, \boldsymbol{Y}$).

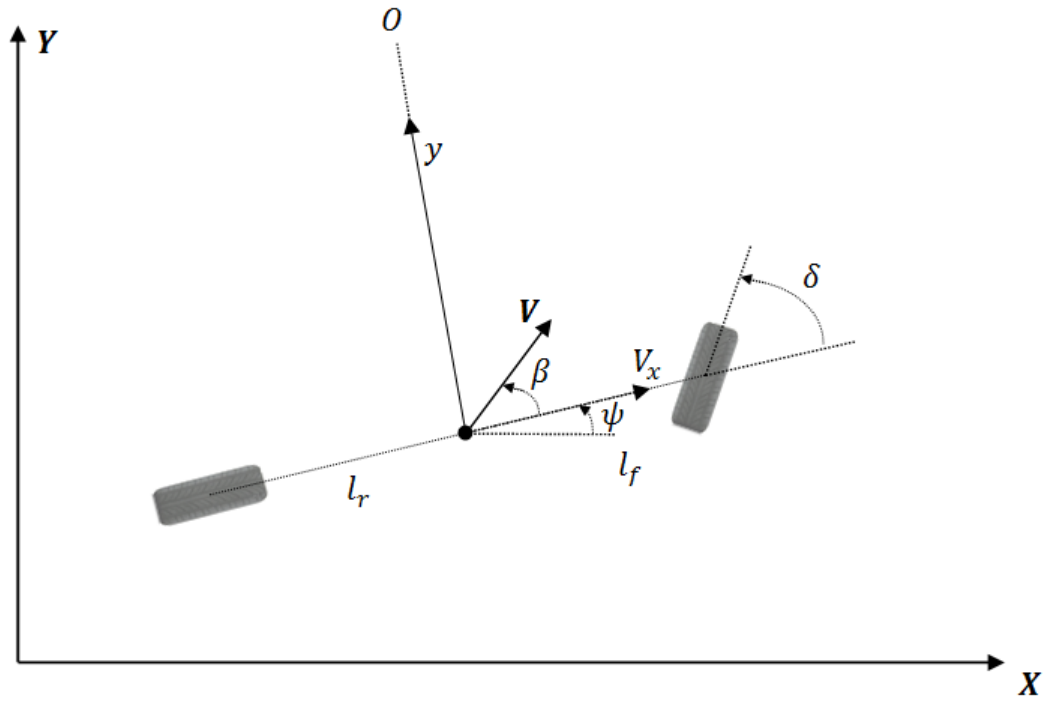

Figure 3.1.1: Lateral vehicle dynamics approximated as a bicycle model

The vehicle yaw-angle ψ is measured as the angle from the global axis $\boldsymbol{X}$ to the vehicle's current orientation, while the lateral position is measured along the lateral axis to the center of rotation of the vehicle. V_x denotes the velocity from the centre of gravity in the direction of

the yaw, while $\boldsymbol{V}$ is the velocity-vector at the centre of gravity. β is the slip-angle at the center of gravity of the vehicle and can be approximated (for sufficiently small angles) as

$$\beta = \dot{y}/V_x \tag{3.1.1}$$

Applying Newton's second law of motion in the y -direction only,

$$ma_y = F_{yf} + F_{yr} \tag{3.1.2}$$

is obtained, where the lateral forces F_{yf} and F_{yr} are those exerted from the front and rear wheels respectively, while a_y denotes the inertial acceleration at the center of gravity in the direction of the y-axis. Decomposing this term further shows that it is the sum of two terms; the lateral acceleration $\ddot{y}$ and the centripetal acceleration $V_x\dot{\psi}$.

Substituting these terms into the left-hand side of equation (3.1.2) yields the following relationship.

$$m\left(\ddot{y} + V_x\dot{\psi}\right) = F_{yf} + F_{yr} \tag{3.1.3}$$

Treating the vehicle as a rod, the moment balance about the z-axis can be formulated similar to that of a beam to obtain the dynamics for the yaw.

$$I_z\ddot{\psi} = l_f F_{yf} - l_r F_{yr} \tag{3.1.4}$$

Here, the constants l_f and l_r denote the distance from the front wheel and rear wheel to the center of gravity, respectively, while I_z is the moment of inertia.

The calculations of the lateral tire forces F_{yf} and F_{yr} involve the slip-angle, and can for small values of this be seen as a proportional relationship. For a more detailed explanation, see [1].

The slip-angle, α, is defined as the difference in the orientation of the tire, δ, and the velocity vector of the front and rear wheel, θ_{Vf} and θ_{Vr} respectively (see figure 3.1.2).

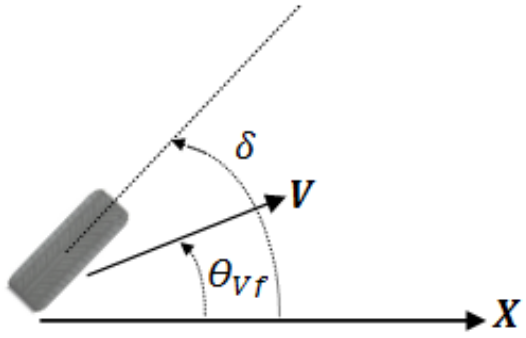

Figure 3.1.2: Illustration of tire-slip angle

Thus, denoting these angles, for the front wheel, α_f (slip angle), δ and θ_{Vf} respectively, it holds that

$$\alpha_f = \delta - \theta_{Vf} \tag{3.1.5}$$

and similarly for the rear wheel

$$\alpha_r = -\theta_{Vr} \tag{3.1.6}$$

since the vehicle does not have rear-wheel steering.

The tire forces are thus formulated as follows, with the cornering stiffness parameters $C_{\alpha f}$ and $C_{\alpha r}$ being the proportionality constants.

$$F_{yf} = 2C_{\alpha f}(\delta - \theta_{Vf}) \tag{3.1.7}$$

$$F_{yr} = 2C_{\alpha r}(-\theta_{Vr}) \tag{3.1.8}$$

The factor of 2 is due to the fact that there are two front wheels and two rear wheels which are lumped together, respectively.

For the tire velocity angles the following relations exist:

$$tan(\theta_{Vf}) = \frac{V_y + l_f\dot{\psi}}{V_x} \tag{3.1.9}$$

$$tan(\theta_{Vr}) = \frac{V_y - l_r\dot{\psi}}{V_x} \tag{3.1.10}$$

Approximating for small angles and substituting the notation $V_y = \dot{y}$, it holds that

$$\theta_{Vf} = \frac{\dot{y} + l_f\dot{\psi}}{V_x} \tag{3.1.11}$$

$$\theta_{Vr} = \frac{\dot{y} - l_r\dot{\psi}}{V_x} \tag{3.1.12}$$

By substituting expressions (3.1.11) and (3.1.12) into (3.1.7) and (3.1.8) respectively, and replacing the results in (3.1.3) and (3.1.4) the following state space model expressing the lateral motion of the vehicle is obtained.

$$\dot{\boldsymbol{x}} = \begin{bmatrix} 0 & 1 & 0 & 0 \\ 0 & -\frac{C_f + C_r}{mV_x} & 0 & -V_x - \frac{C_f l_f - C_r l_r}{mV_x} \\ 0 & 0 & 0 & 1 \\ 0 & -\frac{C_f l_f - C_r l_r}{V_x I_z} & 0 & -\frac{C_f l_f^2 + C_r l_r^2}{V_x I_z} \end{bmatrix} \boldsymbol{x} + \begin{bmatrix} 0 \\ \frac{C_f}{m} \\ 0 \\ \frac{C_f l_f}{I_z} \end{bmatrix} \delta \tag{3.1.13}$$

where $\boldsymbol{x} = [y \quad \dot{y} \quad \psi \quad \dot{\psi}]^T$, $C_f = 2C_{\alpha f}$ and $C_r = 2C_{\alpha r}$.

For analysis and simulation purposes, the parameters presented in Table 3.1.1 were used, where. These correspond to conventional vehicles according to the work done in [5].

Vehicle Parameter	Value
m (mass)	1445 kg
I_z (z-axis inertia)	2094 $kg * m^2$
C_r (cornering stiffness rear)	135200 N/rad
C_f (cornering stiffness front)	135200 N/rad
l_r (distance from CoG to rear axle)	1.79 m
l_f (distance from CoG to front axle)	0.88 m
l_{rb} (distance from CoG to rear bumper)	2.46 m
l_{fb} (distance from CoG to front bumper)	1.54 m

Table 3.1.1: Vehicle parameters

3.2 System Model

With a complete dynamical model of the vehicle obtained, it is of interest to see how the system behaves in the case of following a target vehicle. For the sake of simplification, the leading vehicle is initially modelled as a point at distance L from the centre of gravity of the follower.

Consider the schematic picture below, illustrating two vehicles and their associated orientations. The *lateral deviation*, that is the following car's lateral offset from the target vehicle's position, can be modelled as relations of the two vehicles' states, under the assumption that both vehicles maintain the same longitudinal velocity.

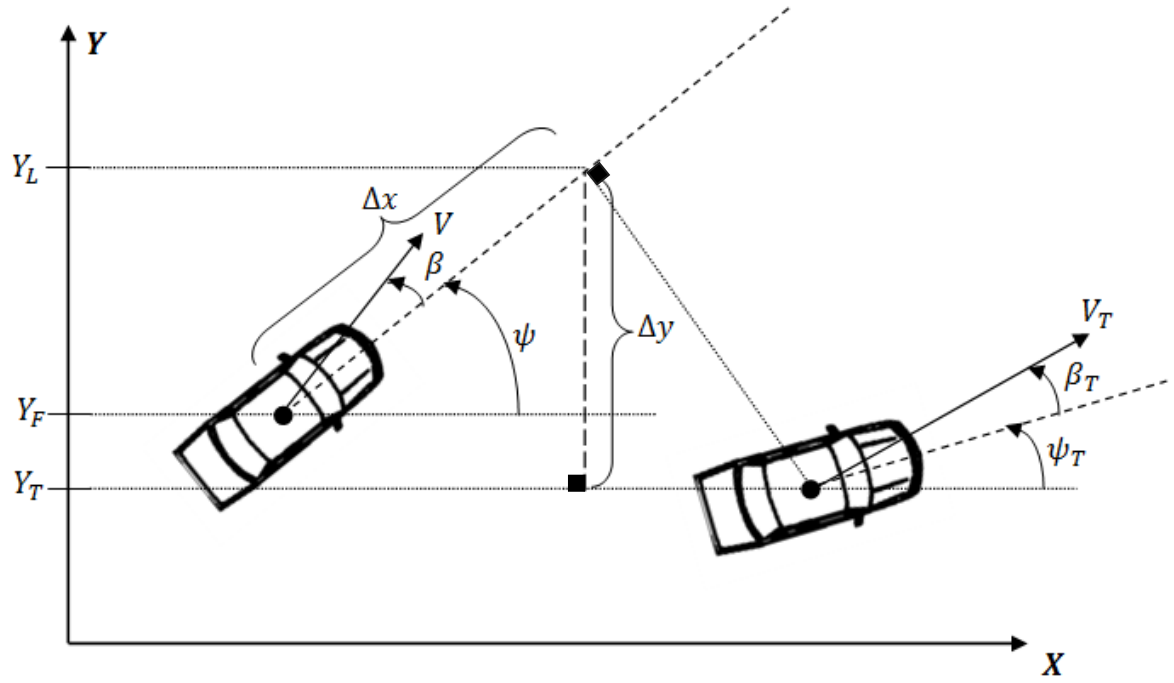

Figure 3.2.1: Geometric interaction of two vehicles

The relation shows that the lateral deviation changes according to the rotation of the following vehicle as well as the difference in the direction of motion of the two vehicles. The indices L, F and T denote $Look-ahead$, $Follower$ and $Target$, respectively. The indices are dropped for the following vehicles states.

By letting Δy be defined as $Y_L - Y_T$, there are two distances to consider; the first being the deviation from centre of gravity to centre of gravity, $Y_F - Y_T$, which is dependent on the distance travelled in the y-direction

$$Y_F(t) - Y_T(t) = V_x \int_{t_0}^{t} (\psi(t) + \beta(t))\, dt - V_x \int_{t_0}^{t} (\psi_T(t) + \beta_T(t))\, dt \qquad (3.2.1)$$

where ψ_T and β_T denote the yaw- and slip-angle of the leading vehicle, respectively, with the assumption of the initial condition for t_0 being no lateral offset.

The second length is from the projected point at a distance Δx from the followers centre of gravity to the centre of gravity of the leading vehicle. This represents the point that is being followed, and can for small deviations be approximated as the look-ahead distance L, as the following figure shows.

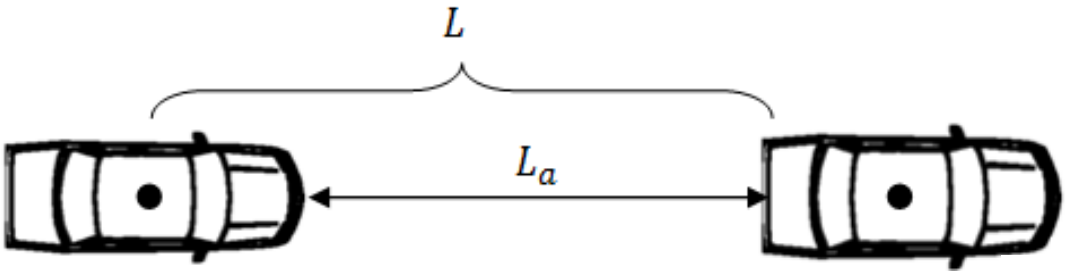

Figure 3.2.2: Representation of look-ahead distance.

$$Y_L(t) - Y_F(t) = L \sin\psi(t) \approx L\psi(t) \qquad (3.2.2)$$

Thus, by approximating for small angles and adding equations (3.2.1) and (3.2.2), the following dynamic equation describing the rate of change of the lateral deviation is obtained.

$$\Delta\dot{y} = L\dot{\psi} + V_x(\psi - \psi_T) + V_x(\beta - \beta_T) \qquad (3.2.3)$$

When augmenting the model described in Section 3.1 with this expression while performing the substitution $\dot{y} = V_x\beta$ as in (3.1.1), the following state-space formulation is obtained, with the state-vector redefined as shown below.

$$\dot{\boldsymbol{x}} = \begin{bmatrix} -\frac{C_r + C_f}{mV_x} & \frac{C_r l_r - C_f l_f}{mV_x^2} - 1 & 0 & 0 \\ \frac{C_r l_r - C_f l_f}{I_z} & -\frac{C_r l_r^2 + C_f l_f^2}{V_x I_z} & 0 & 0 \\ 0 & 1 & 0 & 0 \\ V_x & L & V_x & 0 \end{bmatrix} \boldsymbol{x} + \begin{bmatrix} \frac{C_f}{mV_x} \\ \frac{C_f l_f}{I_z} \\ 0 \\ 0 \end{bmatrix} \delta - \begin{bmatrix} 0 \\ 0 \\ 0 \\ w \end{bmatrix} \qquad (3.2.4)$$

where $\boldsymbol{x} = [\beta \quad \dot{\psi} \quad \psi \quad \Delta y]^T$, $w = V_x(\beta_T + \psi_T)$ and the state y removed since it is of no interest in this case.

In standard form, (3.2.4) can be written as

$$\dot{\boldsymbol{x}} = \boldsymbol{A}\boldsymbol{x} + \boldsymbol{B}\delta \tag{3.2.5}$$

where the matrices $\boldsymbol{A}$ and $\boldsymbol{B}$ are as above and the disturbance vector w ignored.

If instead the point followed is on the rear bumper of the leading vehicle, the expression for w should be modified to

$$w = V_x(\beta_T + \psi_T) - l_{rb}\dot{\psi}_T \tag{3.2.6}$$

where the new term relates the orientation of followed point on the target vehicle's rear bumper. It has to also be noted that the look-ahead distance L can be factored into two parts, a constant part consisting of the distance l_{fb} from the vehicle's center of gravity to the front bumper of the vehicle and a variable term which shall be denoted L_a denoting the distance from the follower's front bumper to the leader's rear bumper, as can be seen in figure 3.2.2.

The term w relates the variations induced by the motions of the leader vehicle; hence, seen from the perspective of the following vehicle, there is no control over it. Treating it as a measured disturbance, the whole system can be visualized in the block-diagram below, where the measured output coming from the sensor is the lateral deviation. Furthermore, $Y_T(t)$ is redefined to include the rear-bumper dynamics, as

$$Y_T(t) = V_x \int_{t_0}^{t} (\psi_T(t) + \beta_T(t))\, dt - l_{rb}\psi_T \tag{3.2.7}$$

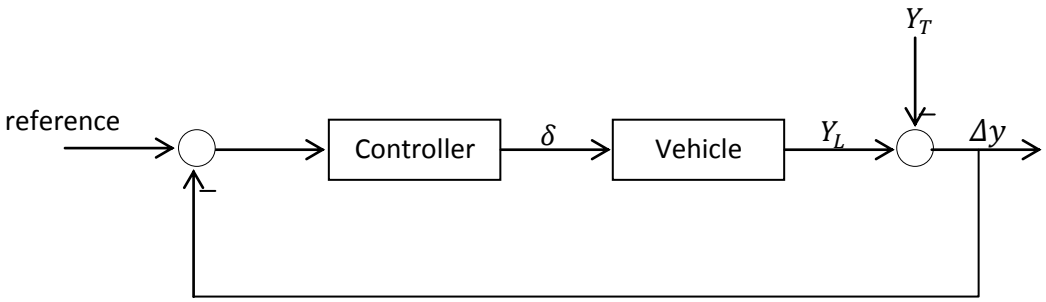

Figure 3.2.3: Block-diagram showing a single-vehicle following system

3.3 Actuator Dynamics

The transfer-function from desired steering-angle to actual angle is dependent on the dynamic of the front wheel steering actuator; it can be seen as dominated by a first-order lag according to [6]. Thus

$$G_{actuator}(s) = \frac{1}{\tau s + 1} \tag{3.3.1}$$

where τ is the time-constant of the motor.

The controller feeds the actuator a desired steering angle, which in turn is converted into the actual steering-profile of the steering-wheel, and finally inputted to the system.

The actuator dynamics can affect the stability margins on the system. Depending on the size of the time-constant, the system might (depending on its characteristics) experience a shift of the crossover frequency to the lower side, as well as a decrease in phase, according to

$$\varphi_{actuator} = -arctan(\omega\tau) \quad (3.3.2)$$

This effect must be taken into consideration when designing a control system for the process – either by including it in the model or by making sure to stay out of its range of operation. The latter can be achieved by tuning the whole system to have a crossover frequency relatively less than the area of effect of the actuator and thus be minimally affected by its amplitude and phase-shift.

4 Analysis

The following chapter is devoted to analysing various characteristics of the system and its behaviour for the parameters which are varying during implementation. It is assumed that the leading vehicle is not moving and hence $Y_T = 0$. The first part consists of frequency-plane bode-analysis while the second part deals with analytical expressions and investigations of the poles and zeros of the system.

4.1 Frequency Analysis

Based on the model introduced in the previous chapter, the transfer-function from the input to the last state Δy is derived as

$$G_{\Delta y}(s) = \boldsymbol{C}(s\boldsymbol{I} - \boldsymbol{A})^{-1}\boldsymbol{B} + \boldsymbol{D} \tag{4.1.1}$$

where $\boldsymbol{C} = [0\ 0\ 0\ 1]$ since the last state is of interest, and $D = 0$. Therefore,

$$G_{\Delta y}(s) = \frac{(e_0 + f_0 L)s^2 + \left(\frac{(b_0 f_0 - d_0 e_0) + (c_0 e_0 - a_0 f_0)L}{V_x}\right)s + (c_0 e_0 - a_0 f_0)}{s^4 - \left(\frac{a_0 + d_0}{V_x}\right)s^3 + \left(\frac{a_0 d_0 - b_0 c_0}{V_x^2} + c_0\right)s^2} \tag{4.1.2}$$

where the varying quantities V_x and L are extracted from the vehicle parameters and the remaining parameters involve quantities that are assumed not to vary at all or negligibly during manoeuvres, such as vehicle mass, cornering stiffness, various lengths, etc.

Thus, the replaced relations are as follows.

$$a_0 = -\frac{C_r + C_f}{m} \tag{4.1.3}$$

$$b_0 = \frac{C_r l_r - C_f l_f}{m} \tag{4.1.5}$$

$$c_0 = \frac{C_r l_r - C_f l_f}{I_z} \tag{4.1.6}$$

$$d_0 = -\frac{C_r l_r^2 + C_f l_f^2}{I_z} \tag{4.1.7}$$

$$e_0 = \frac{C_f}{m} \tag{4.1.8}$$

$$f_0 = \frac{C_f l_f}{I_z} \tag{4.1.9}$$

It is apparent that the varying parameters L and V_x influence the position of the zeros of the system, while V_x in addition to this also moves the poles. These relations are discussed in detail in the next section.

The last state is chosen to be evaluated as it is of interest to control, since the objective is to drive it to zero. Hence, it is of relevance to tailor the open-loop frequency characteristics of this system to maintain desirable margins.

The frequency response of the open-loop plant $G_{\Delta y}(s)$ for different values of the look-ahead distance and longitudinal velocity are shown below in figure 4.1.1. Note that no actuator dynamics are included at this point.

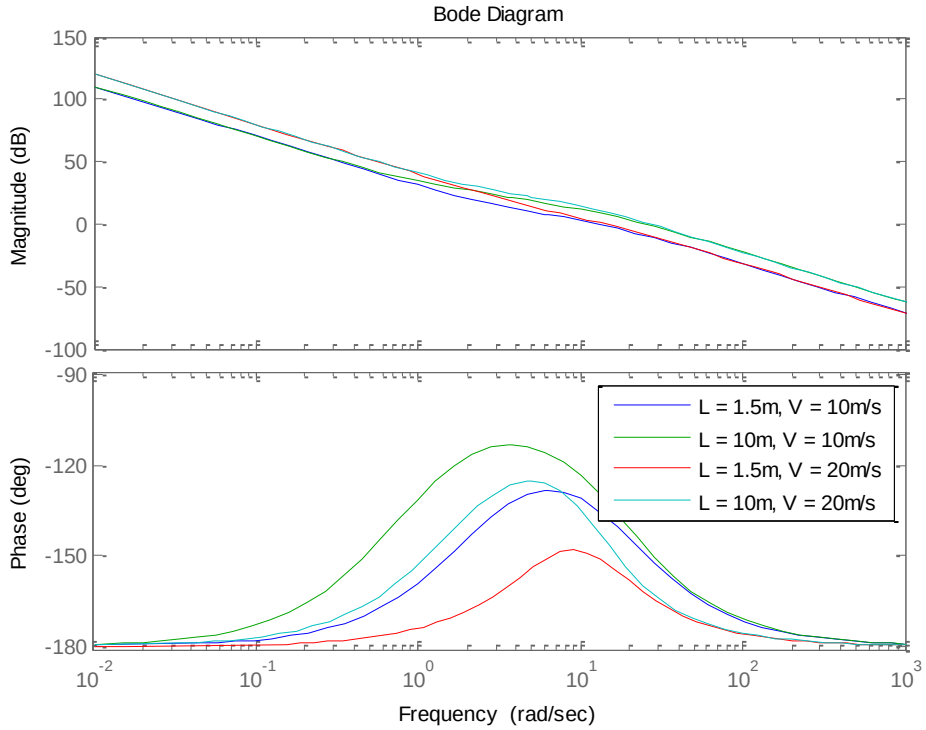

Figure 4.1.1: Open-loop frequency response of system for various look-ahead distances and velocities

It is noted that the system presents different characteristics depending on the velocity and distance to the point followed, and while not unstable, has insufficient phase-margin. The effect is more noticeable for low look-ahead distances and high speed, as will be shown later on. This is augmented when the actuator dynamics with a time-constant of 100ms, described in Section 3.3 are introduced.

The stability margins of the combined system $\frac{G_{\Delta y}(s)}{\tau s+1}$ are shown in figure 4.1.3, for the same look-ahead distances and velocities as in the previous case.

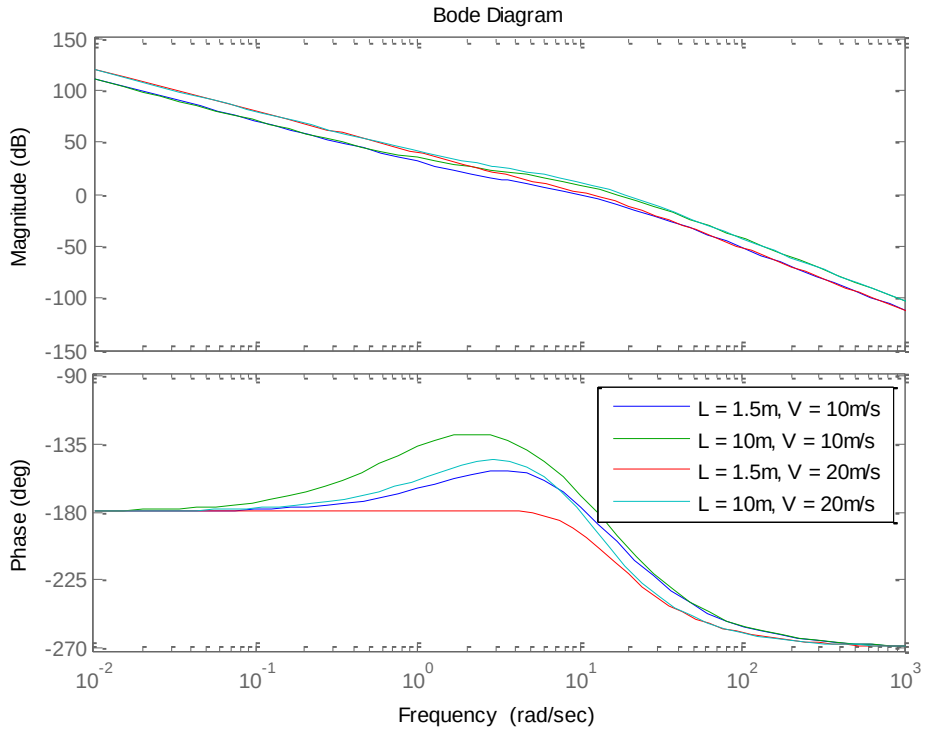

Figure 4.1.2: Open-loop frequency response of system for various look-ahead distances and velocities, with actuator dynamics included

Viewing the plot above it is immediately apparent that the actuator dynamics present a negative effect on the phase-margin. The system is now either unstable or relatively close. Hence, it is in the design of the controller of relevance to shift the crossover frequency of the open-loop system outside the range of the actuator-dynamics, in order to reduce its influence. Furthermore, in the event of delays appearing in the system, it is beneficial to have a low crossover frequency, since the negative phase-contribution of the delay grows linearly with the frequency according to the relation

$$\varphi_d(\omega) = 180\frac{\tau_d \omega}{\pi} \tag{4.1.10}$$

where τ_d is the amount of pure delay in seconds, and φ_d the phase in degrees.

From a control aspect, it is also immediately apparent that a purely proportional controller is not sufficient for the system and a derivative acting part is necessary to raise the phase [7]. Thus, in order to be able to cope under all operating conditions, a PD-controller should be considered at first.

4.2 Pole-Zero Analysis

In this part, analysis of the system's poles and zeros are presented. However, analysis on the coefficients appearing in the transfer function is performed in terms of signs.

Below are listed the coefficients appearing in the transfer-function (4.1.2) and the inequality restrictions associated with them according to the vehicle parameters shown in Table 3.1.1. It should be noted that since the vehicle considered has a length from the centre of gravity to the

rear end of the car which is longer than the distance to the front, the relation $C_r l_r > C_f l_f$ will always hold for the same cornering stiffnesses.

$$(b_0 f_0 - d_0 e_0) = \left(\frac{C_f C_r (l_f + l_r) l_r}{m I_z}\right) > 0 \tag{4.2.1}$$

$$(c_0 e_0 - a_0 f_0) = \left(\frac{C_f C_r (l_r + l_f)}{m I_z}\right) > 0 \Rightarrow (b_0 f_0 - d_0 e_0) = (c_0 e_0 - a_0 f_0) l_r \tag{4.2.2}$$

$$(b_0 f_0 - d_0 e_0) + (c_0 e_0 - a_0 f_0) L = (c_0 e_0 - a_0 f_0) l_r + (c_0 e_0 - a_0 f_0) L = \tag{4.2.3}$$

$$(c_0 e_0 - a_0 f_0)(l_r + L) > 0$$

$$(e_0 + f_0 L) = \left(\frac{I_z C_f + m L C_f l_f}{m I_z}\right) > 0 \tag{4.2.4}$$

$$-(a_0 + d_0) = \frac{C_r \left(I_z + m l_r^2\right) + C_f \left(I_z + m l_f^2\right)}{m I_z} > 0 \tag{4.2.5}$$

$$(a_0 d_0 - b_0 c_0) = \frac{C_r C_f \left(l_r + l_f\right)^2}{m I_z} > 0 \tag{4.2.6}$$

$$(a_0 d_0 - b_0 c_0 + V_x^2 c_0) = \frac{C_r C_f \left(l_r + l_f\right)^2 + m V_x^2 (C_r l_r - C_f l_f)}{m I_z V_x^2} > 0 \tag{4.2.7}$$

4.2.1 Open-Loop Poles

The characteristic equation to be solved is shown below.

$$s^2 \left(s^2 - \left(\frac{a_0 + d_0}{V_x}\right) s + \left(\frac{a_0 d_0 - b_0 c_0}{V_x^2} + c_0\right)\right) = 0 \tag{4.2.1.1}$$

Since the system has a double integrator, two poles appear at the origin. The other two poles are found to be as follows

$$s_{3,4} = \frac{\left(\frac{a_0 + d_0}{V_x}\right) \pm \sqrt{\left(\left(\frac{a_0 + d_0}{V_x}\right)^2 - 4\left(\frac{a_0 d_0 - b_0 c_0}{V_x^2} + c_0\right)\right)}}{2} \tag{4.2.1.2}$$

One interesting factor to consider is when the poles go from being purely real into a complex pair. Since it is known from (4.2.1.7) that the second term in the square-root expression is always positive, the following condition on V_x can be derived for the poles to be complex.

$$V_x > \sqrt{\frac{(a_0 - d_0)^2 + 4 b_0 c_0}{4 c_0}} \tag{4.2.1.3}$$

Thus, for the vehicle considered, the following inequality should hold for the open-loop poles to be complex.

$V_x > 10.2879$ m/s

The following figure shows how the poles move for all velocities V_x ranging from 5m/s to 50m/s.

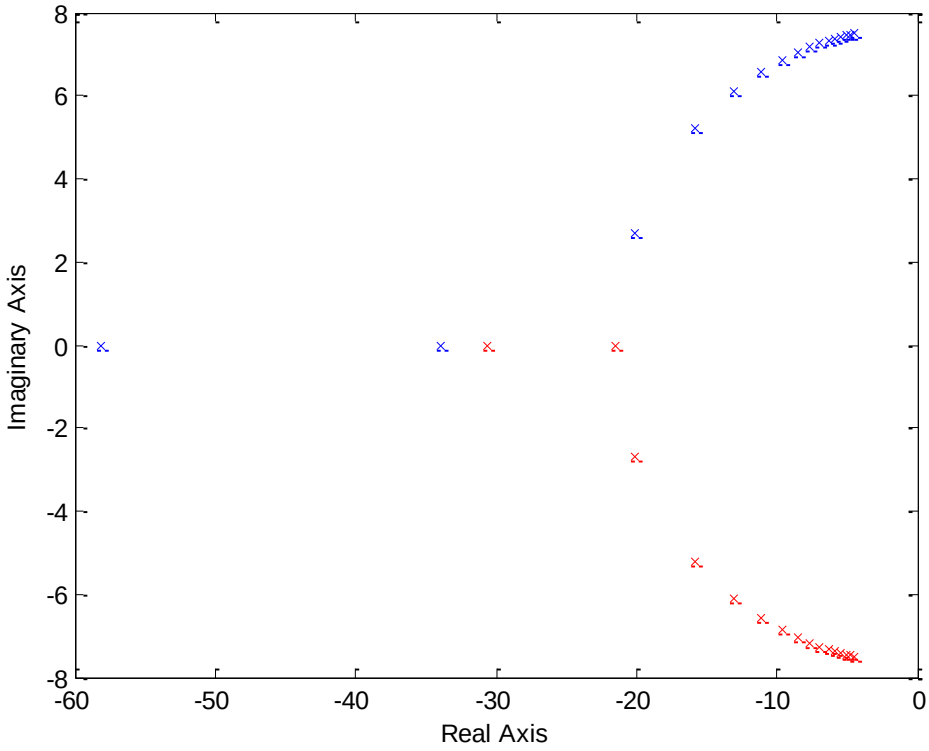

Fig 4.2.1.1: Open-loop plant poles moving from left to right and becoming complex as the velocity is increased.

4.2.2 Open-Loop Zeros

The equation to be solved is as follows

$$(e_0 + f_0 L)s^2 + \left(\frac{(c_0 e_0 - a_0 f_0)(L + l_r)}{V_x}\right) s + (c_0 e_0 - a_0 f_0) = 0 \qquad (4.2.2.1)$$

The solution would then be

$$s = \frac{-\left(\frac{(c_0 e_0 - a_0 f_0)(L + l_r)}{V_x}\right) \pm \sqrt{\left(\left(\frac{(c_0 e_0 - a_0 f_0)(L + l_r)}{V_x}\right)^2 - 4(e_0 + f_0 L)(c_0 e_0 - a_0 f_0)\right)}}{2(e_0 + f_0 L)} \qquad (4.2.2.2)$$

The system will have complex zeros based on the values of V_x and L. Thus, the system will have complex zeros under the following condition.

$$V_x > \sqrt{\frac{(c_0 e_0 - a_0 f_0)(l_r + L)^2}{4(e_0 + f_0 L)}} \qquad (4.2.2.3)$$

The following figure shows the relation where the equality holds.

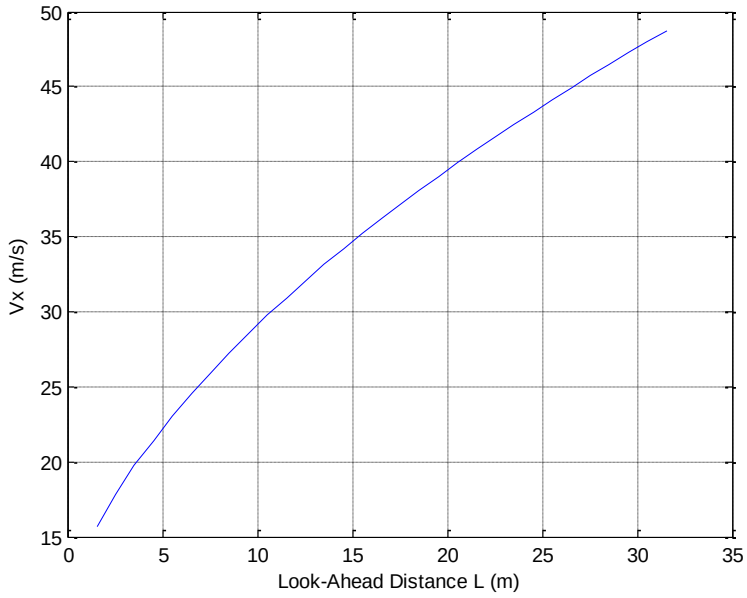

Fig. 4.2.2.1: The crossing point where the zeros of the system turn complex, with the lower half belonging to the real region, and the upper to the complex.

The following figure shows how the zeros move for look-ahead distances ranging from 1.54m to 31.54m, with a velocity of 25m/s. It is consistent with the figure introduced previously; when the look-ahead is increased, the zeros go from complex to purely real.

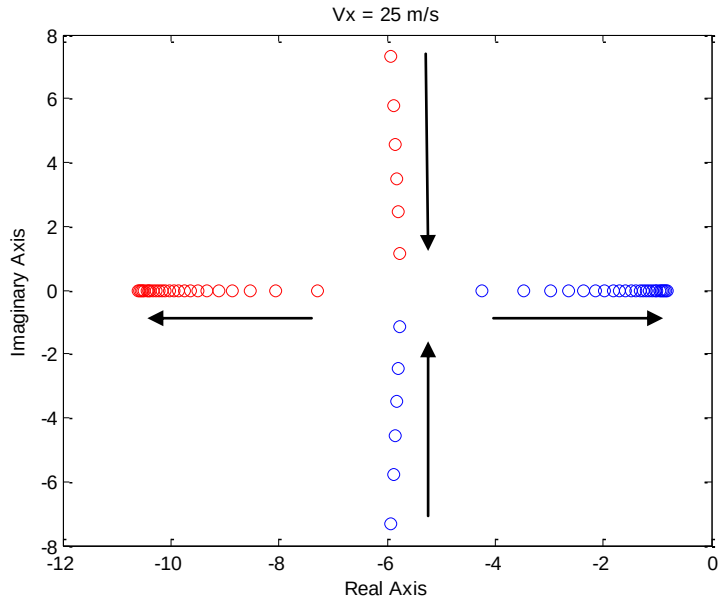

Fig. 4.2.2.2: The movement of the open-loop zeros as the look-ahead is increased.

Thus it can be seen that the system exhibits multiple characteristics depending on the operating range; for low look-ahead distances and high velocities the plant presents inherent complex poles.

5 Control Design

This chapter will describe the various approaches that were made in the control design and the assumptions and limitations of each.

The aim of the controller is to stabilize the two-vehicle following system, meaning that the follower should be able to follow the leading vehicle. The nature of the problem is that the car is bounded in the lateral direction by the lane it is within. Thus, the step response of the follower should ideally be an over-damped response. If not possible, then the overshoot should be as small as possible. Another important factor is that the rise time of the response should be acceptable, preferably within one second. Lastly, the settling time of the response should not be very long.

From the previous chapter it was concluded that a purely proportional controller is not enough to stabilize the plant, and thus there is a need to increase complexity.

A conventional PID-controller can be formulated as

$$u(t) = K_p e(t) + K_i \int_0^t e(\tau)d\tau + K_d \frac{d}{dt} e(t) \tag{5.1}$$

where K_p is the proportional gain, K_i the integral gain, K_d the derivative gain and $e(t)$ the error signal acted upon [8]. The corresponding transfer-function from error to control-signal would thus be

$$F_{PID}(s) = \frac{U(s)}{E(s)} = K_p + \frac{K_i}{s} + K_d s = \frac{K_d s^2 + K_p s + K_i}{s} \tag{5.2}$$

However, in this case the integral part is not necessary due to the inherit integration in the plant, and hence the controller takes on the form of a Proportional-Derivative (PD) controller.

5.1 PD-Controller

Since there are no sensor measurements available for the rate of change of the lateral error, a filtered PD controller is used. The filter is used to reduce the influence of high frequency noise [8]. The controller is therefore of the following form

$$F_{PD}(s) = K_p \left(1 + \frac{T_d s}{1 + T_f s}\right) = K_p \frac{(1 + \tau_d s)}{\left(1 + \frac{\tau_d s}{b}\right)} \tag{5.1.1}$$

where the following relations were used for the last equality.

$$\tau_d = T_d + T_f \tag{5.1.2}$$

$$b = \frac{\tau_d}{T_f} \tag{5.1.3}$$

Since the aim is to increase the open-loop phase margin, the tuning method will be similar to that of a lead compensator. The following rules govern how to tune the controller to a desired phase margin ϕ_m at a desired crossover frequency ω_c :

1) Determine the gain $\left|G_p(i\omega_c)\right|$ and phase $arg\, G_p(i\omega_c)$ of the plant at the desired frequency ω_c .
2) Determine how much phase-margin increase is needed from the following equation:

$$\phi_{increase} = \phi_m - arg\, G_p(i\omega_c) + \pi \tag{5.1.3}$$

3) Calculate the parameter b from the following relation:

$$b = \frac{1+sin(\phi_{increase})}{1-sin(\phi_{increase})} \tag{5.1.4}$$

4) Next, obtain τ_d from the following relation:

$$\tau_d = \frac{\sqrt{b}}{\omega_c} \tag{5.1.5}$$

5) Finally, calculate the proportional gain K_p as follows:

$$K_p = \frac{1}{\sqrt{b}*|G_p(i\omega_c)|} \tag{5.1.6}$$

This simple method gives the user freedom to choose the crossover frequency and phase-margin that is desired. For a simple second order system, there is a direct relationship between crossover frequency and rise-time [9]. However, since this system is of more complex nature, only approximate relations can be made regarding the rise-time.

5.2 PDD-Controller

Next, another derivative was added to the controller for an extra degree of freedom when performing pole placement design and to possibly achieve better performance. The controller takes on the following form.

$$F_{PDD}(s) = K_p\left(1 + \frac{T_v s}{(T_{f_1}s+1)} + \frac{T_a s^2}{(T_{f_1}s+1)(T_{f_2}s+1)}\right) \tag{5.2.1}$$

$$= \frac{K_p\left(\left(T_a + T_v T_{f_2} + T_{f_1} T_{f_2}\right)s^2 + \left(T_v + T_{f_1} + T_{f_2}\right)s + 1\right)}{(T_{f_1}s+1)(T_{f_2}s+1)}$$

The formulation above can be rewritten as:

$$F_{PDD}(s) = K_p' \frac{(T_1 s+1)(T_2 s+1)}{(T_{f_1}s+1)(T_{f_2}s+1)} \tag{5.2.2}$$

It can be seen from (5.2.2) that the compensator resembles two cascaded PD-controllers. Since the aim is to increase the open-loop gain to a desired value, depending on how the poles and zeros of the controller are placed, it has the capability of adding up to 180° phase margin. This property is especially good when the system might have time delays as it can provide higher tolerance to higher delays compared to a PD-controller while maintaining the desired performance. The tuning can be achieved by cascading two lead filters where each of them contributes by adding a part of the desired open-loop phase margin. This method can add up

to 180 degrees of additional phase at a desired crossover frequency. The tuning rules for the lead filter are similar to those described for the PD controller.

Thus, the controller can be rewritten in this form

$$F_{PDD}(s) = K_p \frac{(1+\tau_{d_1}s)}{\left(1+\frac{\tau_{d_1}s}{b_1}\right)} \frac{(1+\tau_{d_2}s)}{\left(1+\frac{\tau_{d_2}s}{b_2}\right)} = K_p * Lead_1(s) * Lead_2(s) \quad (5.2.3)$$

With having to tune two lead filters, the question becomes how to choose the amount of phase each of them should contribute to the desired open-loop phase margin. Since the aim is to only increase the phase to values less than 90 degrees, the following rules are considered.

1) The first lead controller is used to increase the open-loop phase margin to half of the desired phase margin. Thus,
   $$\phi_{increase1} = \frac{\phi_m}{2} - arg\, G_p(i\omega_c) + \pi \quad (5.2.4)$$
2) Then, the second lead filter compensates for the rest of the desired phase.
   $$\phi_{increase2} = \frac{\phi_m}{2} \quad (5.2.5)$$
3) The proportional gain is chosen such that the crossover frequency is at the desired point.
   $$K_p = \frac{1}{\sqrt{b_1}*\sqrt{b_2}*|G_p(i\omega_c)|} \quad (5.2.6)$$

5.3 Pole-Placement Design

For pole placement requirements, a higher order controller is needed to correctly place all poles as desired (actuator dynamics ignored). The controller has the following form:

$$F_{PD^3}(s) = \frac{T_3s^3+T_2s^2+T_1s+T_0}{s^3+T_{f2}s^2+T_{f1}s+T_{f0}} \quad (5.3.1)$$

This controller has 7 tuning parameters and rather than using it for open-loop frequency design (there are too many tuning parameter for two requirements), it will be solely used for closed-loop pole placement. Although the actuator dynamics are ignored in the pole placement, it will have an impact on the results of the pole placement.

The poles are placed in a pattern similar to those of resulting from the PD-controller explained in Section 5.1. However, there exist three extra poles which are placed purely real. Since the positioning of 7 poles in relation to 5 zeros is rather difficult to motivate in terms of overshoot, rise-time or other parameters of relevance, the placements were determined through rigorous testing. The investigations were conducted with an initial look-ahead distance and longitudinal velocity of 1.5m and 10m/s, respectively. Thus, by modifying the pole-positions as these parameters were increased, a relevant tuning law was sought.

As seen in equation (4.2.2.2) explained in Section 4.2, the zeros of the plant will move closer to the imaginary axis with the increase of velocity. Therefore, the damping of the dominant complex conjugate poles is tuned to increase proportionally. This is equivalent with letting

their angle to the real axis decrease linearly with the velocity. Furthermore, it was deemed necessary to increase the radius of the three dominant poles at higher velocities. It was noted that pulling the dominant poles to the left also moved the zeros in the same direction. If uncompensated for, a pair of complex zeros will dominate the system at high speeds and low look-ahead distances and lead to poor performance. This resulted in the first tuning rule described below.

$$\frac{Vx}{30} < r_1, r_2, r_3 < 2 - \frac{Vx}{30} \tag{5.3.2}$$

where r_i, $i = 1,2,3$, is the radius of the poles p_1, p_2, p_3. The angle from the real axis can be chosen as

$$\phi = 40 - Vx/1.5 \tag{5.3.3}$$

The next pair of complex poles were placed similarly, albeit with a real part depending on the ratio $\frac{d_1}{2*d_2}$ (which is the real part of the complex conjugate zeros of the plant), where

$$d_1 = b_o f_o - d_o e_o + \frac{c_0 * e_o - a_o * f_0}{Vx} \tag{5.3.4}$$

$$d_2 = e_0 + f_0 \tag{5.3.5}$$

and an imaginary component making the damping similar to that of the first pair of complex poles, but changing with a ratio of $15/V_x$.

Thus, the real part of the poles can be chosen as

$$-\frac{d_1}{2*d_2} - 5 < real(p_4, p_5) < -\frac{d_1}{2*d_2} - 4 \tag{5.3.6}$$

Let the damping of the complex poles determined in (5.3.2) and (5.3.3) be

$$damp_{p_{1,2}} = real(p_{1,2}) / \sqrt{real(p_{1,2}) + Im(p_{1,2})} \tag{5.3.7}$$

Then, to achieve a similar damping for the poles in (5.3.6), however with a ratio of $15/V_x$, the imaginary component should be chosen as

$$Im(p_{4,5}) = \frac{\sqrt{real(p_{4,5})^2 \left(damp_{p_{1,2}}^2 + 1\right)}}{damp_{p_{1,2}}^2} \frac{V_x}{15} \tag{5.3.8}$$

The real pole is placed such that

$$-\frac{d_1}{2*d_2} - 6 < p_6 < -\frac{d_1}{2*d_2} \tag{5.3.9}$$

holds.

The last remaining pole was moved far to the left, basically to ignore its dynamics.

$$p_7 = -25 \tag{5.3.10}$$

The poles' positions will change as the look-ahead distance and velocity changes; this change in operating region will in turn lead to the zeros of the plant moving as well. Thus it cannot be expected for the same position to perform the same for every operating region. These restrictions will, once combined, define a region in which poles can be placed to yield relatively consistent behaviour for a large range of look-ahead distances and velocities. However, it should be noted that once the actuator is implemented, the poles will not remain in their original positions. The experiments presented in Section 7.4 were nevertheless performed with the actuator included.

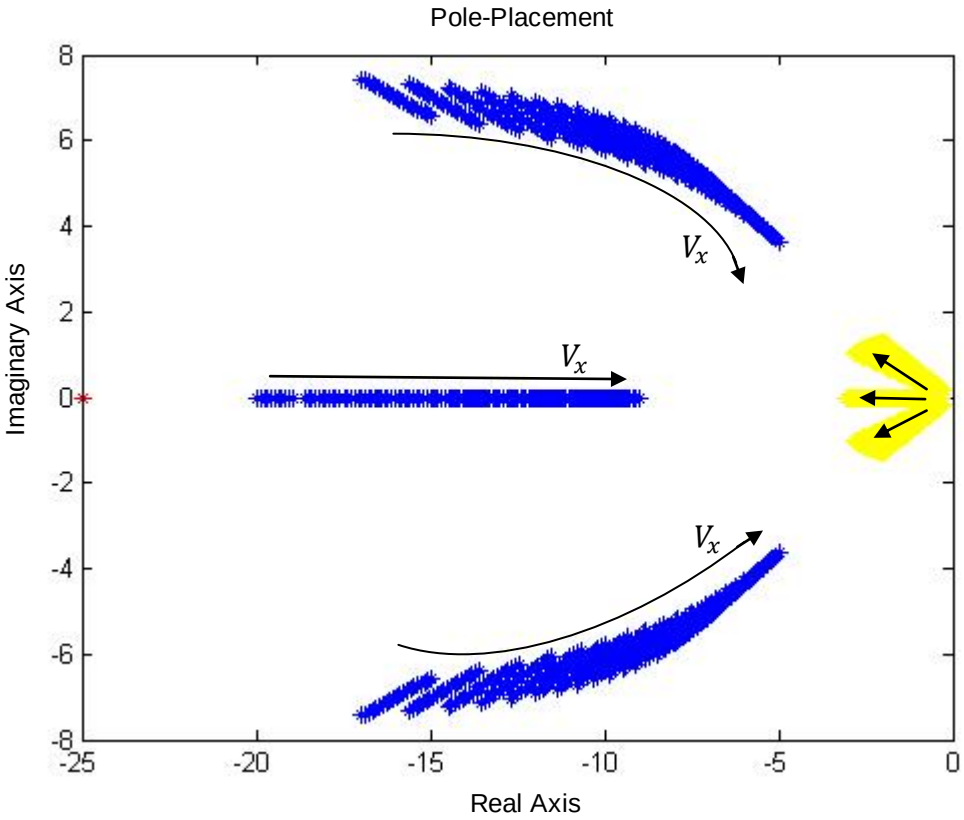

Figure 5.3.2: Plot of the movement of poles according to the rules set above, as the velocity is varied between 10m/s to 30m/s, and the look-ahead distance between 1m and 15m.

5.4 State Feedback

In this section, both full state feedback and output feedback are discussed along with the limitations introduced by considering the actuator dynamics. The system is shown in its state-space form in (3.2.5).

5.4.1 Full State Feedback

Normal state feedback can be written in the following form

$$u(t) = -\boldsymbol{K} * \boldsymbol{x} \tag{5.4.1.1}$$

where $\boldsymbol{K}$ is the feedback gain matrix. However, in the system considered, full-state feedback with reference following is derived. Hence, the controller is written as follows.

$$u = -\boldsymbol{K} * \left(\boldsymbol{x} - \boldsymbol{x_{ref}}\right) = -[K_1 \quad K_2 \quad K_3 \quad K_4] * \left(\boldsymbol{x} - \boldsymbol{x_{ref}}\right) \tag{5.4.1.2}$$

where K_1, K_2, K_3, K_4 are the feedback gains and $\boldsymbol{x_{ref}}$ is the vector of references to the states.

Thus, the system (3.2.5) can be rewritten as

$$\dot{\boldsymbol{x}} = \boldsymbol{A'} * \boldsymbol{x} + \boldsymbol{B'} * \boldsymbol{x_{ref}} \tag{5.4.1.3}$$

where

$$\boldsymbol{A'} = \boldsymbol{A} - \boldsymbol{B} * \boldsymbol{K} = \begin{bmatrix} \frac{a_0}{V_x} - \frac{e_0}{V_x}K_1 & (\frac{b_0}{V_x^2} - 1) & -\frac{e_0}{V_x}K_2 & -\frac{e_0}{V_x}K_3 & -\frac{e_0}{V_x}K_4 \\ c_0 - f_0K_1 & \frac{d_0}{V_x} - f_0K_2 & & -f_0K_3 & -f_0K_4 \\ 0 & 1 & & 0 & 0 \\ V_x & L & & V_x & 0 \end{bmatrix} \tag{5.4.1.4}$$

and

$$\boldsymbol{B'} = \boldsymbol{B} * \boldsymbol{K} = \begin{bmatrix} \frac{e_0}{V_x}K_1 & \frac{e_0}{V_x}K_2 & \frac{e_0}{V_x}K_3 & \frac{e_0}{V_x}K_4 \\ f_0K_1 & f_0K_2 & f_0K_3 & f_0K_4 \\ 0 & 0 & 0 & 0 \\ 0 & 0 & 0 & 0 \end{bmatrix} \tag{5.4.1.5}$$

The poles of the closed-loop system are the eigenvalues of the $\boldsymbol{A'}$ matrix. The characteristic equation is written as follows.

$$s^4 + \left(\frac{-a_0 - d_0 + K_1e_0}{V_x} + K_2f_0\right)s^3$$

$$+ \left(\frac{a + bK_1}{V_x^2} + K_2\left(\frac{c}{V_x}\right) - K_1f_0 + K_3f_0 + K_4(e_0 + f_0L) + c_0\right)s^2 \tag{5.4.1.6}$$

$$+ \left(\left(K_3 + K_4(L + l_r)\right)\left(\frac{c}{V_x}\right)\right)s + (cK_4)$$

where $a = (a_0d_0 - b_0c_0)$, $b = (b_0f_0 - d_0e_0)$ and $c = (c_0e_0 - a_0f_0)$.

Suppose the poles are to be placed such that the characteristic equation of the closed-loop system is written in the following form:

$$\prod_{j=1}^{n}(s + p_j) = 0 \tag{5.4.1.7}$$

Then, by expanding (5.4.1.7) and equating it to (5.4.1.6), the following sets of equations have to be satisfied to place all the poles at the desired locations.

$$\begin{cases} cK_4 = p_1p_2p_3p_4 \\ \frac{c}{V_x}\left(K_3 + K_4(L + l_r)\right) = p_1p_2(p_3 + p_4) + p_3p_4(p_1 + p_2) \\ \frac{a+bK_1}{V_x^2} + K_2\left(\frac{c}{V_x}\right) - K_1f_0 + K_3f_0 + K_4(e_0 + f_0L) + c_0 = p_1p_2 + p_3p_4 + p_1p_3 + p_1p_4 + p_2p_3 + p_2p_4 \\ \frac{-a_0-d_0}{V_x} + \frac{K_1e_0}{V_x} + K_2f_0 = p_1 + p_2 + p_3 + p_4 \end{cases}$$

(5.4.1.8)-(5.4.1.11)

where $Re\{p_j\} > 0 \ \forall j$ has to be satisfied for stability.

Since there are four variables and four equations, there is a unique solution for the gain vector $\boldsymbol{K}$. Next, the actuator dynamics are considered which will lead to having the system's order increase to five instead of four. The dynamics are introduced as follows.

$$\frac{\delta(s)}{u(s)} = \frac{1}{\tau s+1} \tag{5.4.1.12}$$

Performing an inverse Laplace-transform yields

$$u = \tau\dot{\delta} + \delta \tag{5.4.1.13}$$

$$u = -\boldsymbol{K} * \left(\boldsymbol{x} - \boldsymbol{x_{ref}}\right) \tag{5.4.1.14}$$

Equating the two previous equations yields

$$\dot{\delta} = -\frac{\delta}{\tau} - \frac{1}{\tau}\boldsymbol{K} * \boldsymbol{x} + \frac{1}{\tau}\boldsymbol{K} * \boldsymbol{x_{ref}} \tag{5.4.1.15}$$

Thus, the new extended state space equations can be written as:

$$\frac{d}{dt}\begin{pmatrix}\boldsymbol{x}\\ \delta\end{pmatrix} = \begin{bmatrix}\boldsymbol{A} & \boldsymbol{B}\\ -\frac{1}{\tau}\boldsymbol{K} & -\frac{1}{\tau}\end{bmatrix}\begin{pmatrix}\boldsymbol{x}\\ \delta\end{pmatrix} + \begin{bmatrix}0_{4x4} & 0_{4x1}\\ \frac{1}{\tau}\boldsymbol{K} & 0\end{bmatrix}\begin{pmatrix}\boldsymbol{x_{ref}}\\ \delta\end{pmatrix} = \boldsymbol{A}^* * \begin{pmatrix}\boldsymbol{x}\\ \delta\end{pmatrix} + \boldsymbol{B}^* * \begin{pmatrix}\boldsymbol{x_{ref}}\\ \delta\end{pmatrix} \tag{5.4.1.16}$$

where

$$\boldsymbol{A}^* = \begin{bmatrix} \frac{a_0}{V_x} & \left(\frac{b_0}{V_x^2} - 1\right) & 0 & 0 & \frac{e_0}{V_x} \\ c_0 & \frac{d_0}{V_x} & 0 & 0 & f_0 \\ 0 & 1 & 0 & 0 & 0 \\ V_x & L & V_x & 0 & 0 \\ -\frac{K_1}{\tau} & -\frac{K_2}{\tau} & -\frac{K_3}{\tau} & -\frac{K_4}{\tau} & -\frac{1}{\tau} \end{bmatrix} \tag{5.4.1.17}$$

and

$$\boldsymbol{B}^* = \begin{bmatrix} 0 & 0 & 0 & 0 & 0 \\ 0 & 0 & 0 & 0 & 0 \\ 0 & 0 & 0 & 0 & 0 \\ 0 & 0 & 0 & 0 & 0 \\ \frac{K_1}{\tau} & \frac{K_2}{\tau} & \frac{K_3}{\tau} & \frac{K_4}{\tau} & 0 \end{bmatrix} \tag{5.4.1.18}$$

The poles of the closed-loop system are the eigenvalues of the $\mathbf{A}^*$ matrix. The characteristic equation is as follows:

$$s^5 + \left(\frac{-a_0 - d_0}{V_x} + \frac{1}{\tau}\right)s^4 \quad + \left(\frac{K_1 e_0}{\tau V_x} + \frac{K_2 f_0}{\tau} + \frac{1}{\tau}\left(\frac{-a_0 - d_0}{V_x}\right) + \frac{a}{V_x^2} + c_0\right)s^3$$

$$+ \left(\frac{a+bK_1}{\tau V_x^2} - \frac{K_1 f_0}{\tau} + K_2\left(\frac{c}{\tau V_x}\right) + \frac{K_3 f_0}{\tau} + \frac{K_4}{\tau}(e_0 + f_0 L) + \frac{1}{\tau}c_0\right)s^2 \qquad (5.4.1.19)$$

$$+ \left(\left(K_3 + K_4(L + l_r)\right)\left(\frac{c}{\tau V_x}\right)\right)s + \left(\frac{cK_4}{\tau}\right) = 0$$

where τ is the time constant of the actuator. As can be seen, the system to be solved can be written as in (5.4.1.8)-(5.4.1.11) with one important distinction; when the poles are chosen, the following condition must always hold:

$$\frac{-a_0 - d_0}{V_x} + \frac{1}{\tau} = p_1 + p_2 + p_3 + p_4 + p_5 \qquad (5.4.1.20)$$

that is, the sum of all the poles is fixed.

Full state feedback has not been considered so far since it was not possible to gain access to all the states. Hence, the output feedback approach was considered.

5.4.2 Output Feedback

The outputs of interest are the yaw-rate and the lateral deviation, since these are measurable.

$$\boldsymbol{y} = \boldsymbol{C} * \boldsymbol{x} = \begin{bmatrix} 0 & 1 & 0 & 0 \\ 0 & 0 & 0 & 1 \end{bmatrix} * \boldsymbol{x} \qquad (5.4.2.1)$$

The controller is written as follows.

$$u = -\boldsymbol{K} * (\boldsymbol{y} - \boldsymbol{y_{ref}}) = -[K_2 \quad K_4] * \begin{bmatrix} 0 & 1 & 0 & 0 \\ 0 & 0 & 0 & 1 \end{bmatrix} * \left(\boldsymbol{x} - \boldsymbol{x_{ref}}\right)$$

$$= -\boldsymbol{K'} * \left(\boldsymbol{x} - \boldsymbol{x_{ref}}\right) = -[0 \quad K_2 \quad 0 \quad K_4] * \left(\boldsymbol{x} - \boldsymbol{x_{ref}}\right) \qquad (5.4.2.2)$$

As can be seen, it is equivalent to setting K_1 and K_3 to zero. Thus, the system matrices are the same as in (5.4.1.17) and (5.4.1.18) but with $K_1 = 0$ and $K_3 = 0$. Hence, the characteristic equation can be written as follows

$$s^5 + \left(\frac{-a_0 - d_0}{V_x} + \frac{1}{\tau}\right)s^4 \quad + \left(\frac{K_2 f_0}{\tau} + \frac{1}{\tau}\left(\frac{-a_0 - d_0}{V_x}\right) + \frac{a}{V_x^2} + c_0\right)s^3$$

$$+ \left(\frac{a}{\tau V_x^2} + K_2\left(\frac{c}{\tau V_x}\right) + \frac{K_4}{\tau}(e_0 + f_0 L) + \frac{1}{\tau}c_0\right)s^2 \qquad (5.4.2.3)$$

$$+ \left(K_4(L + l_r)\left(\frac{c}{\tau V_x}\right)\right)s + \left(\frac{cK_4}{\tau}\right) = 0$$

Other that the limitation expressed by (5.4.1.20), it can be seen that there are more equations than variables and hence exact pole placement is not possible. The solution for the set of equations will yield dominating poles that are always complex as will be shown in Section 7.1.

Next, the rate of change and acceleration of the lateral deviation were estimated from their definitions shown below.

$$\Delta\dot{y} = L\dot{\psi} + V_x\psi + V_x\beta = L\dot{\psi} + disturbance \tag{5.4.2.4}$$

$$\Delta\ddot{y} = L\ddot{\psi} + V_x\dot{\psi} + V_x\dot{\beta} = V_x\dot{\psi} + disturbance \tag{5.4.2.5}$$

to include only the yaw-rate while the rest of the terms were lumped as disturbances. Thus, the expressions reduce to the following.

$$\Delta\dot{y} = L\dot{\psi} \tag{5.4.2.6}$$

and

$$\Delta\ddot{y} = V_x\dot{\psi} \tag{5.4.2.7}$$

This approach was tested to see if it would add one more degree of freedom for pole placement. The output of the system is now described by

$$\boldsymbol{y} = \boldsymbol{C} * \boldsymbol{x} = \begin{bmatrix} 0 & L & 0 & 0 \\ 0 & V_x & 0 & 0 \\ 0 & 0 & 0 & 1 \end{bmatrix} * \boldsymbol{x} \tag{5.4.2.8}$$

As can be seen, the rank of the output matrix $\boldsymbol{C}$ is still two, which means that and hence the problem is the same as before. It will only add redundancy to the characteristic equation with no added flexibility in placing several poles.

6 String Stability

After stabilizing the two cars following system, it is of interest to look at the stability of a platoon of vehicles. The concept of string-stability is of great of importance once extending the two-vehicle model into a platoon with an arbitrary number of vehicles n, and has been discussed in great detail by researchers, however mostly longitudinal string stability (see [10] and [11]). If the case is such that the lateral error from the first follower propagates back and is amplified, it can lead to vehicles further down the platoon cutting corners or leaving the lane due to too large errors. Thus, it is of significance to investigate and verify whether a platoon is string-stable or not.

6.1 Definition of String Stability

Let $y_e^{(i)}(t)$ denote the measured lateral error from vehicle i to vehicle $i-1$, in [12] and [13]

A platoon of n vehicles is said to be string stable in the L_2 norm sense if for every $i \in [2, n]$, the relation $\left\| y_e^{(i)}(t) \right\|_2 < \left\| y_e^{(i-1)}(t) \right\|_2$ holds.

If string-stability holds, a disturbance in the system will always attenuate as it propagates throughout the platoon. This approach is different from the one discussed in [12] and [13], where the L_∞ norm is considered instead of the L_2 norm. That former approach imposes a condition on the infinity norm $\|H(j\omega)\|_\infty$ as well as having the sign of the impulse response of $H(j\omega)$ be non-changing which proved to be difficult to analyse. A translation of the definition above to the frequency domain would mean that if the transfer function from the error of a vehicle to that of its following vehicle has a magnitude less than 1, string stability is ensured. Thus, the condition is that

$$\|H(j\omega)\|_\infty = \left\| \frac{\varepsilon_i(j\omega)}{\varepsilon_{i-1}(j\omega)} \right\|_\infty < 1 \Rightarrow \left| \frac{\varepsilon_i(j\omega)}{\varepsilon_{i-1}(j\omega)} \right| < 1 \ \forall \omega \tag{6.1.1}$$

holds, where $\varepsilon_i(j\omega)$ denotes the Laplace transform of the lateral error $y_e^{(i)}(t)$ from vehicle i to the preceding vehicle, and $\varepsilon_{i-1}(j\omega)$ similarly from vehicle $i-1$ to its preceding vehicle. The requirement is therefore that the infinity norm $\|H(j\omega)\|_\infty$ is strictly less than one.

In order to investigate whether the system is string stable or not, proper error functions must be determined. Hence, since the error would in this case be the lateral deviation, the following relations are set up.

Let the error from vehicle i to vehicle $i-1$ be defined as the projected lateral offset from the center of gravity of the following vehicle to the rear bumper of the leader, as defined in (3.2.3) where

$$\begin{aligned} \dot{y}_e^{(i)} &= \Delta\dot{y}_i = L\dot{\psi}_i + V_x\psi_i + V_x\beta_i - V_x\psi_{i-1} - V_x\beta_{i-i} + l_{rb}\dot{\psi}_{i-1} \\ &= \left(L\dot{\psi}_i + V_x\psi_i + V_x\beta_i\right) - \left(-l_{rb}\dot{\psi}_{i-1} + V_x\psi_{i-1} + V_x\beta_{i-i}\right) \end{aligned} \tag{6.1.2}$$

where the term $l_{rb}\dot{\psi}_{i-1}$ is introduced from following the rear bumper given by (3.2.7) Since every vehicle in the platoon is assumed to be identical and thus having the same controller acting on the lateral error, the control signal for vehicle i can be written as $u_i = -C\varepsilon_i$ where C is the controller used by the vehicle. It is assumed at this point that there is no communication between the vehicles in the platoon. Thus, by performing a Laplace transform, the previous relation can be rewritten as

$$s * \varepsilon_i = \left(LG_{\dot{\psi}_i} + V_x G_{\psi_i} + V_x G_{\beta_i}\right)u_i - \left(-l_{rb}G_{\dot{\psi}_{i-1}} + V_x G_{\psi_{i-1}} + V_x G_{\beta_{i-1}}\right)u_{i-1} \qquad (6.1.3)$$

Since it has been assumed that all the vehicles are identical, $G_{\dot{\psi}_i} = G_{\dot{\psi}_{i-1}}$ must hold and similarly for the rest of the expressions. Hence, the indices can be omitted and the relation can be written as

$$\varepsilon_i = \frac{\left(LG_{\dot{\psi}} + V_x G_{\psi} + V_x G_{\beta}\right)}{s}u_i - \frac{\left(-l_{rb}G_{\dot{\psi}} + V_x G_{\psi} + V_x G_{\beta}\right)}{s}u_{i-1} \qquad (6.1.4)$$

where the expression $\frac{\left(LG_{\dot{\psi}} + V_x G_{\psi} + V_x G_{\beta}\right)}{s}$, similar to that in (4.1.2) can be written as $G_{\Delta y}$, whereas the other expression $\frac{\left(-l_{rb}G_{\dot{\psi}} + V_x G_{\psi} + V_x G_{\beta}\right)}{s}$ represents the dynamics of the movement of the point on the rear bumper that is to be tracked by the sensor. It is similar to that of $G_{\Delta y}$ but with L replaced by $-l_{rb}$ and will for distinction be denoted G_{rb}.

$$G_{\Delta y}(s) = \frac{(e_0 + f_0 L)s^2 + \left(\frac{(c_0 e_0 - a_0 f_0)(L + l_r)}{V_x}\right)s + (c_0 e_0 - a_0 f_0)}{s^4 - \left(\frac{a_0 + d_0}{V_x}\right)s^3 + \left(\frac{a_0 d_0 - b_0 c_0}{V_x^2} + c_0\right)s^2} \qquad (6.1.5)$$

$$G_{rb}(s) = \frac{(e_0 - f_0 l_{rb})s^2 + \left(\frac{(c_0 e_0 - a_0 f_0)(-l_{rb} + l_r)}{V_x}\right)s + (c_0 e_0 - a_0 f_0)}{s^4 - \left(\frac{a_0 + d_0}{V_x}\right)s^3 + \left(\frac{a_0 d_0 - b_0 c_0}{V_x^2} + c_0\right)s^2} \qquad (6.1.6)$$

The relation in (6.4) can therefore be written as

$$\varepsilon_i = G_{\Delta y}u_i - G_{rb}u_{i-1} \qquad (6.1.7)$$

By substituting for the control signals the relation can be written as

$$\varepsilon_i = G_{\Delta y}u_i - G_{rb}u_{i-1} = G_{\Delta y}(-C\varepsilon_i) - G_{rb}(-C\varepsilon_{i-1}) \qquad (6.1.8)$$

Thus, the ratio of the errors can finally be written as follows.

$$\frac{\varepsilon_i}{\varepsilon_{i-1}} = \frac{G_{rb}C}{1 + G_{\Delta y}C} \qquad (6.1.9)$$

A couple of remarks on the expression (6.9) have to be taken into consideration:

- G_{rb} and $G_{\Delta y}$ share the same poles and only differ in their zeros.
- At steady-state, $\frac{G_{rb}C}{1+G_{\Delta y}C}$ and $\frac{G_{\Delta y}C}{1+G_{\Delta y}C}$ are the same.

From the remarks above, it is clear that at best when the system is controlled to achieve an over-damped response, the ratio will be $\left\| \frac{\varepsilon_i(j\omega)}{\varepsilon_{i-1}(j\omega)} \right\|_\infty \leq 1$ with equality. It means that for low frequencies, the error will propagate equally along the platoon. In the case where the controlled system experiences overshoot, that overshoot will propagate down the platoon causing the error to grow with respect to the leader. Although all vehicles will converge to the path of the leader eventually, the system is bound by the lane it is moving within and should not move unnecessarily in the lateral direction since it might cause the cars to cross into the other lanes. Thus, for the decentralized platoon, it should hold that the controlled system should not have any overshoot at all.

Next, inter-vehicle communication is considered where feed-forward from previous vehicles in the platoon is conveyed down the platoon. The figure below shows how the feed-forward information is fed to the system, where F is the feed-forward filter.

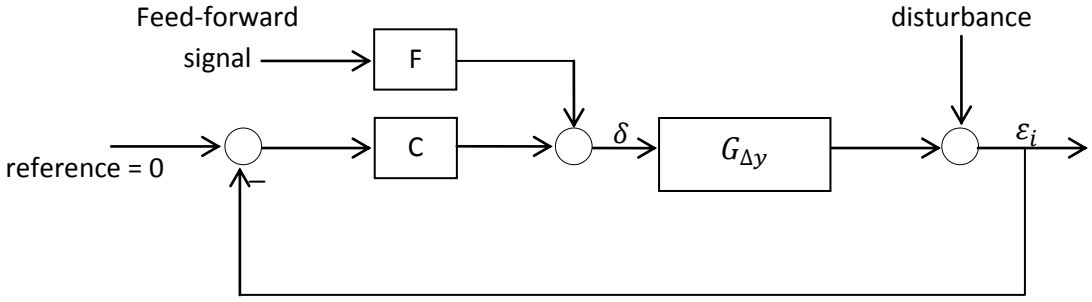

Figure 6.1: Illustrative picture of feed-forward from previous vehicles.

Different topologies for vehicle communication along with their limitations are introduced. Four different approaches are presented along with their assumptions and information streams required.

6.2 Information from Preceding Vehicle Only

In this part, the lateral deviation of the preceding vehicle is transmitted to the vehicle immediately following it, as illustrated in the figure below.

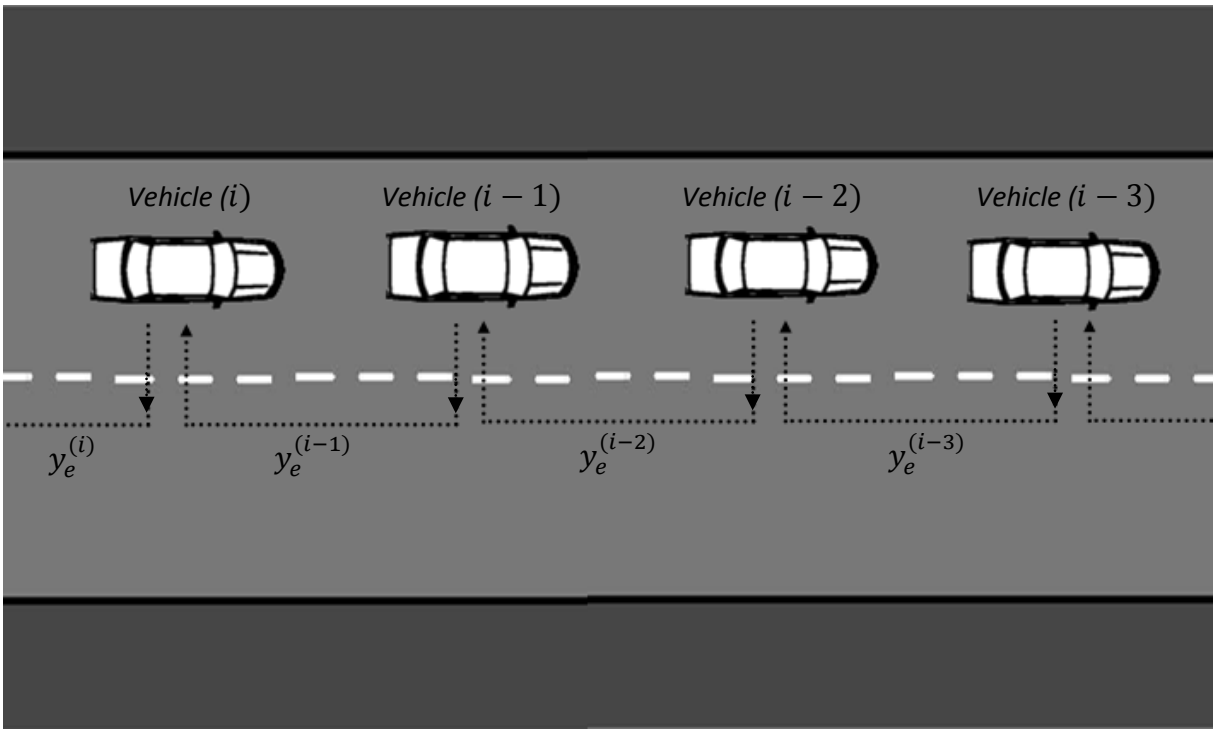

Figure 6.2.1: Illustrative picture of first communication topology considered.

The control signals for vehicles i and $i-1$ are defined as follows

$$u_i = -C\varepsilon_i + F\varepsilon_{i-1} \tag{6.2.1}$$

$$u_{i-1} = -C\varepsilon_{i-1} + F\varepsilon_{i-2} \tag{6.2.2}$$

where F is the feed-forward filter and is assumed to be the same for all followers. Substituting the signals in (6.1.7) the relation between the errors can be written as

$$\begin{aligned}\varepsilon_i &= G_{\Delta y}u_i - G_{rb}u_{i-1} \\ &= G_{\Delta y}(-C\varepsilon_i + F\varepsilon_{i-1}) - G_{rb}(-C\varepsilon_{i-1} + F\varepsilon_{i-2}) \\ &= -G_{\Delta y}C\varepsilon_i + G_{\Delta y}F\varepsilon_{i-1} + G_{rb}C\varepsilon_{i-1} - G_{rb}F\varepsilon_{i-2}\end{aligned} \tag{6.2.3}$$

Grouping the similar error terms yields

$$(1 + G_{\Delta y}C)\varepsilon_i = (G_{\Delta y}F + G_{rb}C)\varepsilon_{i-1} - G_{rb}F\varepsilon_{i-2} \tag{6.2.4}$$

The relation above cannot be written as a simple ratio of the lateral errors between only vehicles i and $i-1$ and is dependent on follower $i-2$. The unwanted term from follower $i-2$ prevents making any conclusion about string stability. Simulation results using this approach are shown in Section 7.6.

6.3 Information from All Preceding Vehicles

In this part, the sum of the lateral deviations from all the preceding vehicles is transmitted to the i^{th} vehicle. After adding more information from previous vehicles, it was found that there is a possibility to eliminate the appearance of lateral error terms other than those of the

immediate preceding vehicle by communicating the sum of the lateral deviations from all the preceding vehicles. Consider the figure below showing a part of a platoon.

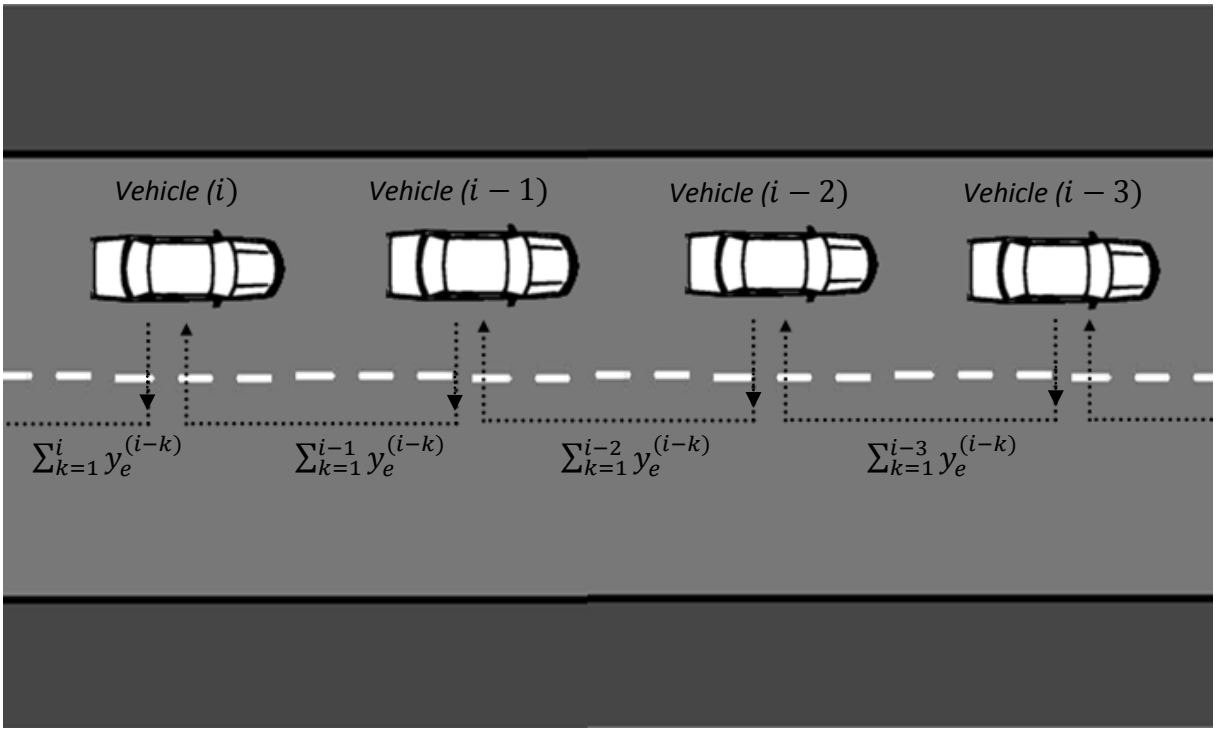

Figure 6.3.1: Illustrative picture of the second communication topology considered.

The control signals for vehicles i and $i-1$ are defined as follows

$$u_i = -C\varepsilon_i + F\left(\sum_{k=1}^{i-1} \varepsilon_{i-k}\right) = -C\varepsilon_i + F(\varepsilon_{i-1} + \varepsilon_{i-2} + \cdots) \tag{6.3.1}$$

$$u_{i-1} = -C\varepsilon_{i-1} + F\left(\sum_{k=2}^{i-1} \varepsilon_{i-k}\right) = -C\varepsilon_i + F(\varepsilon_{i-2} + \varepsilon_{i-3} + \cdots) \tag{6.3.2}$$

where F is the feed-forward filter. Substituting the signals in (6.1.7), the relation between the errors can be written as follows.

$$\varepsilon_i = G_{\Delta y} u_i - G_{rb} u_{i-1}$$

$$= G_{\Delta y}\left(-C\varepsilon_i + F(\varepsilon_{i-1} + \varepsilon_{i-2} + \cdots)\right) - G_{rb}\left(-C\varepsilon_{i-1} + F(\varepsilon_{i-2} + \varepsilon_{i-3} + \cdots)\right) \tag{6.3.3}$$

$$= -G_{\Delta y} C\varepsilon_i + G_{\Delta y} F\varepsilon_{i-1} + G_{\Delta y} F(\varepsilon_{i-2} + \varepsilon_{i-3} + \cdots) + G_{rb} C\varepsilon_{i-1} - G_{rb} F(\varepsilon_{i-2} + \varepsilon_{i-3} + \cdots)$$

Grouping the similar error terms yields

$$\left(1 + G_{\Delta y} C\right)\varepsilon_i = \left(G_{\Delta y} F + G_{rb} C\right)\varepsilon_{i-1} + F(G_{\Delta y} - G_{rb})(\varepsilon_{i-2} + \varepsilon_{i-3} + \cdots) \tag{6.3.4}$$

As in the previous case, the relation above is dependent on previous vehicles and cannot be written as a simple ratio of the lateral errors between only vehicles i and $i-1$. However, under the condition that

$$G_{\Delta y} = G_{rb} = G \tag{6.3.5}$$

the ratio of the errors can be simplified and written as

$$\frac{\varepsilon_i}{\varepsilon_{i-1}} = \frac{G(C+F)}{1+GC} \ \forall i \tag{6.3.6}$$

By choosing $F = k * C$ where k is a constant, the ratio becomes

$$\frac{\varepsilon_i}{\varepsilon_{i-1}} = \frac{GC(k+1)}{1+GC} \ \forall \tag{6.3.7}$$

By making a correct choice of k, string stability of a platoon of n vehicles can be achieved by having

$$\left|\frac{\varepsilon_i}{\varepsilon_{i-1}}\right| = \left|\frac{GC(k+1)}{1+GC}\right| < 1 \ \forall \omega \tag{6.3.8}$$

Next, the conditions under which $G_{\Delta y} = G_{rb}$ holds are discussed.

6.3.1 Conditions for String Stability

For the equality condition (6.3.5) on $G_{\Delta y}$ and G_{rb} to hold, their corresponding expressions have to be evaluated.

$$G_{\Delta y}(s) = \frac{(e_0+f_0L)s^2+\left(\frac{(c_0e_0-a_0f_0)(L+l_r)}{V_x}\right)s+(c_0e_0-a_0f_0)}{s^4-\left(\frac{a_0+d_0}{V_x}\right)s^3+\left(\frac{a_0d_0-b_0c_0}{V_x^2}+c_0\right)s^2} \tag{6.3.1.1}$$

$$G_{rb}(s) = \frac{(e_0-f_0l_{rb})s^2+\left(\frac{(c_0e_0-a_0f_0)(-l_{rb}+l_r)}{V_x}\right)s+(c_0e_0-a_0f_0)}{s^4-\left(\frac{a_0+d_0}{V_x}\right)s^3+\left(\frac{a_0d_0-b_0c_0}{V_x^2}+c_0\right)s^2} \tag{6.3.1.2}$$

Thus, for the equality condition to hold, it should hold that $-l_{rb}G_{\dot{\psi}} = LG_{\dot{\psi}} = 0$. There are two ways to make sure it holds. First, the term $-l_{rb}G_{\dot{\psi}}$ is introduced because of following the rear bumper and can be made to disappear by following the vehicle's centre of gravity instead, or by set-point manipulation. Thus, it is possible to write G_{rb} as follows

$$G_{rb} = \frac{(e_0)s^2+\left(\frac{(c_0e_0-a_0f_0)(l_r)}{V_x}\right)s+(c_0e_0-a_0f_0)}{s^4-\left(\frac{a_0+d_0}{V_x}\right)s^3+\left(\frac{a_0d_0-b_0c_0}{V_x^2}+c_0\right)s^2} \tag{6.3.1.3}$$

Next, it has to be made that the look-ahead term is set to zero. One way to do so is to set $L = 0$ which would lead to $LG_{\dot{\psi}} = 0$. This is called the look-down scheme as defined in Section 2.1. By manipulation of the lateral error sensor measurements, it is possible to emulate the movements of the vehicle with respect to the path of the previous vehicle and control the system as if it were operating based on a look-down scheme. Under these assumptions, string stability is guaranteed for a platoon of vehicles regardless of how many vehicles are in the platoon. However, having a system of this kind of situation is no different than having a lane following algorithm and the concept of a platoon does not hold anymore.

The other way is to assume that the vehicles exhibit no yaw-movement and moves in the y-direction only. This would yield that $-l_{rb}G_{\dot{\psi}} = LG_{\dot{\psi}} = 0$. The results of this approach will be discussed in Section 7.6.

6.3.2 If Equality Assumption Does Not Hold

If the assumption (6.3.5) does not hold for the system, the only way to get rid of the unwanted terms in (6.3.4) is to let the feed-forward filter F be defined as a function of every vehicle. Thus, in this case the assumption that all vehicles have the same feed-forward filter does not hold however they do have the same controller C.

The control signals in (6.3.1) and (6.3.2) are then rewritten as follows

$$u_i = -C\varepsilon_i + F_i(\varepsilon_{i-1} + \varepsilon_{i-2} + \cdots) \tag{6.3.2.1}$$

$$u_{i-1} = -C\varepsilon_{i-1} + F_{i-1}(\varepsilon_{i-2} + \varepsilon_{i-3} + \cdots) \tag{6.3.2.2}$$

which results in the change of (6.2.3) to the following relation.

$$\begin{aligned}\varepsilon_i &= G_{\Delta y}u_i - G_{rb}u_{i-1} \\ &= G_{\Delta y}\big(-C\varepsilon_i + F_i(\varepsilon_{i-1} + \varepsilon_{i-2} + \cdots)\big) - G_{rb}\big(-C\varepsilon_{i-1} + F_{i-1}(\varepsilon_{i-2} + \varepsilon_{i-3} + \cdots)\big) \\ &= -G_{\Delta y}C\varepsilon_i + G_{\Delta y}\big(F_i\varepsilon_{i-1} + F_i(\varepsilon_{i-2} + \varepsilon_{i-3} + \cdots)\big) + G_{rb}\big(C\varepsilon_{i-1} - F_{i-1}(\varepsilon_{i-2} + \varepsilon_{i-3} + \cdots)\big)\end{aligned} \tag{6.3.2.3}$$

yielding

$$\big(1 + G_{\Delta y}C\big)\varepsilon_i = \big(G_{\Delta y}F_i + G_{rb}C\big)\varepsilon_{i-1} + (G_{\Delta y}F_i - G_{rb}F_{i-1})(\varepsilon_{i-2} + \varepsilon_{i-3} + \cdots) \tag{6.3.2.4}$$

The next step is to rewrite $G_{\Delta y}$ and G_{rb} as the ratio of their respective polynomials as follows.

$$G_{\Delta y} = \frac{(e_0 + f_0L)s^2 + \left(\frac{(c_0e_0 - a_0f_0)(L + l_r)}{V_x}\right)s + (c_0e_0 - a_0f_0)}{s^4 - \left(\frac{a_0 + d_0}{V_x}\right)s^3 + \left(\frac{a_0d_0 - b_0c_0}{V_x^2} + c_0\right)s^2} = \frac{A_{\Delta y}}{B} \tag{6.3.2.5}$$

$$G_{rb} = \frac{(e_0 - f_0l_{rb})s^2 + \left(\frac{(c_0e_0 - a_0f_0)(-l_{rb} + l_r)}{V_x}\right)s + (c_0e_0 - a_0f_0)}{s^4 - \left(\frac{a_0 + d_0}{V_x}\right)s^3 + \left(\frac{a_0d_0 - b_0c_0}{V_x^2} + c_0\right)s^2} = \frac{A_{rb}}{B} \tag{6.3.2.6}$$

where $A_{\Delta y}$ and A_{rb} are the polynomials representing the zeros of $G_{\Delta y}$ and G_{rb} respectively. Substituting the expressions in the right-hand side of (6.3.2.4) yields

$$\big(1 + G_{\Delta y}C\big)\varepsilon_i = \frac{1}{B}\big(A_{\Delta y}F_i + A_{rb}C\big)\varepsilon_{i-1} + \frac{1}{B}(A_{\Delta y}F_i - A_{rb}F_{i-1})(\varepsilon_{i-2} + \varepsilon_{i-3} + \cdots) \tag{6.3.2.7}$$

for $i \geq 2$. To find a suitable selection for the filter for each follower, analysis on the error ratios from every vehicle to the next starting from the second follower has to be done.

For the second follower, the expression (6.3.2.7) is written as follows.

$$\big(1 + G_{\Delta y}C\big)\varepsilon_2 = \frac{1}{B}\big(A_{\Delta y}F_2 + A_{rb}C\big)\varepsilon_1 \tag{6.3.2.8}$$

Thus, a suitable choice of the filter F_2 would be

$$F_2 = k * C * \frac{A_{rb}}{A_{\Delta y}} \tag{6.3.2.9}$$

where k is a constant. Thus, the ratio of the second follower's lateral error to the first follower becomes

$$\frac{\varepsilon_2}{\varepsilon_1} = \frac{G_{rb}C(k+1)}{(1+G_{\Delta y}C)} \tag{6.3.2.10}$$

Similarly as in (6.3.8), k can be selected such that the infinity norm of the ratio can be forced to be less than one. Next, for the third follower, the expression (6.3.2.7) is written as follows.

$$(1 + G_{\Delta y}C)\varepsilon_3 = \frac{1}{B}(A_{\Delta y}F_3 + A_{rb}C)\varepsilon_2 + \frac{1}{B}(A_{\Delta y}F_3 - A_{rb}F_2)\varepsilon_1 \tag{6.3.2.11}$$

For the influence on the error from the first follower to disappear, a suitable choice of the filter F_3 would be

$$F_3 = \frac{A_{rb}}{A_{\Delta y}}F_2 = k * C * \left(\frac{A_{rb}}{A_{\Delta y}}\right)^2 \tag{6.3.2.12}$$

By substituting in (6.3.2.11), the term involving ε_1 would disappear. Thus, the ratio of the third follower's lateral error to the second follower becomes

$$\frac{\varepsilon_3}{\varepsilon_2} = \frac{G_{rb}C\left(k\left(\frac{A_{rb}}{A_{\Delta y}}\right)+1\right)}{(1+G_{\Delta y}C)} \tag{6.3.2.13}$$

For the general case, by letting the feed-forward filter for follower $i \geq 2$ be chosen as

$$F_i = \frac{A_{rb}}{A_{\Delta y}}F_{i-1} = k * C * \left(\frac{A_{rb}}{A_{\Delta y}}\right)^{i-1} \tag{6.3.2.14}$$

and substituting into (6.3.2.7), the following relation is derived

$$(1 + G_{\Delta y}C)\varepsilon_i = \frac{C}{B}\left(A_{\Delta y}k\left(\frac{A_{rb}}{A_{\Delta y}}\right)^{i-1} + A_{rb}\right)\varepsilon_{i-1} \; = G_{rb}C\left(k\left(\frac{A_{rb}}{A_{\Delta y}}\right)^{i-2} + 1\right)\varepsilon_{i-1} \tag{6.3.2.15}$$

Thus, the ratio of the error from the follower i to follower $i-1$ can be written as follow

$$\frac{\varepsilon_i}{\varepsilon_{i-1}} = \frac{G_{rb}C\left(k\left(\frac{A_{rb}}{A_{\Delta y}}\right)^{i-2}+1\right)}{(1+G_{\Delta y}C)} \tag{6.3.2.16}$$

Disadvantages of using this approximation are

- The feed-forward filter is a function of the vehicle's order in the platoon.
- The feed-forward filter increases in complexity with the vehicle's position in the platoon, order $2,4,6,8 \ldots 2(i-1)$ where i is the vehicle's order in the platoon.

- The ratio is dependent on the operating conditions of the platoon in terms of look-ahead distance and longitudinal velocity and thus the number of vehicles guaranteed to maintain string stability might change depending on the operating points.

This approach is discarded due to the reasons mentioned above and will be discussed further in Section 7.6.

Along with the approaches mentioned above, two more have been investigated to eliminate the need for selecting the filter depending on the vehicles position in the platoon. Due to a pending patent, they cannot be presented here and can be referred to through patent number, I2828SE00.

7 Simulation Results

In this section, the results of tuning the controllers according to the rules introduced previously are presented and discussed. Long runs have been made for variations of the desired tuning parameters and thereafter the effects these parameters have on the step response of the system are discussed.

7.1 Output Feedback

A few runs have been made by varying the gains K_2 and K_4 from 0.01 to 25. The following plots shows how the poles move with the varying gains in both cases of ignoring and including the actuator dynamics.

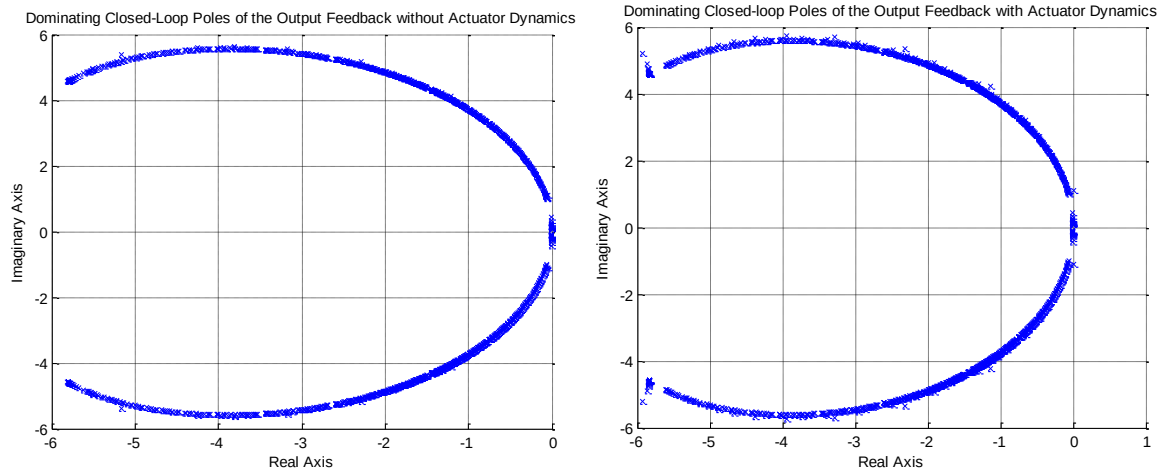

Figures 7.1-7.2: Plots of the dominating poles as feedback-gains are increased, without actuator and with, respectively.

As can be seen, there is no way the dominating poles can be placed all real and hence an over-damped response cannot be achieved.

7.2 PD-Controller

Long runs have been made over the values of L_a from 0 to 30 meters, V_x from 0 to 50m/s (or 0 – 180km/h) and desired phase-margin from 40 to 89 degrees. Each run was conducted with setting the desired crossover frequency to a fixed value. The results displayed below are for the crossover frequencies of 1 and 2rad/s. The design criteria are as mentioned in the beginning of chapter 5.

First, a look at the minimum overshoot achieved for a given crossover frequency and the phase margins under which they are achieved along with the rise-time for the responses is desired. The figures below show the results.

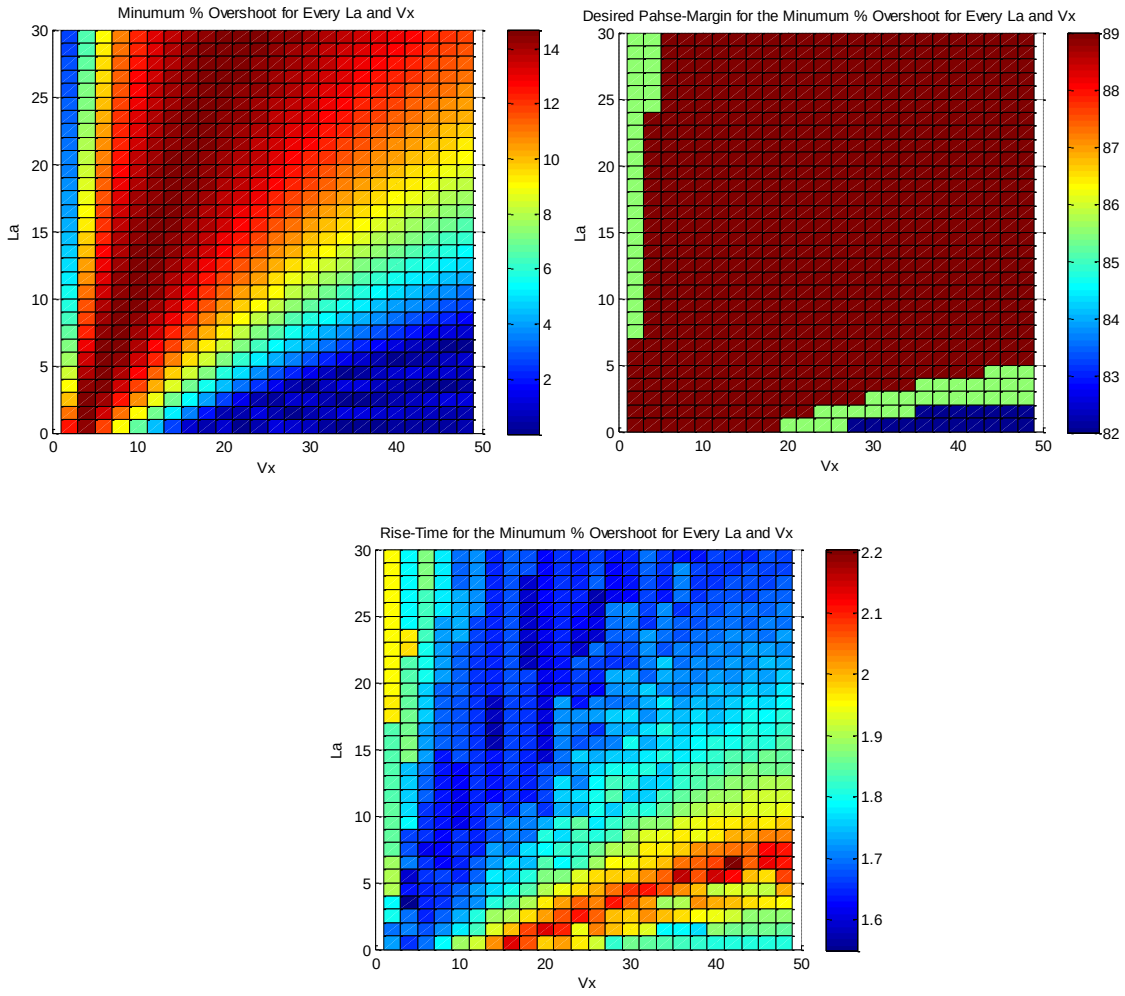

Figures 7.2.1-7.2.3: Plots of minimum overshoot, its associated phase-margin and rise-time, respectively for a crossover frequency of 1rad/s.

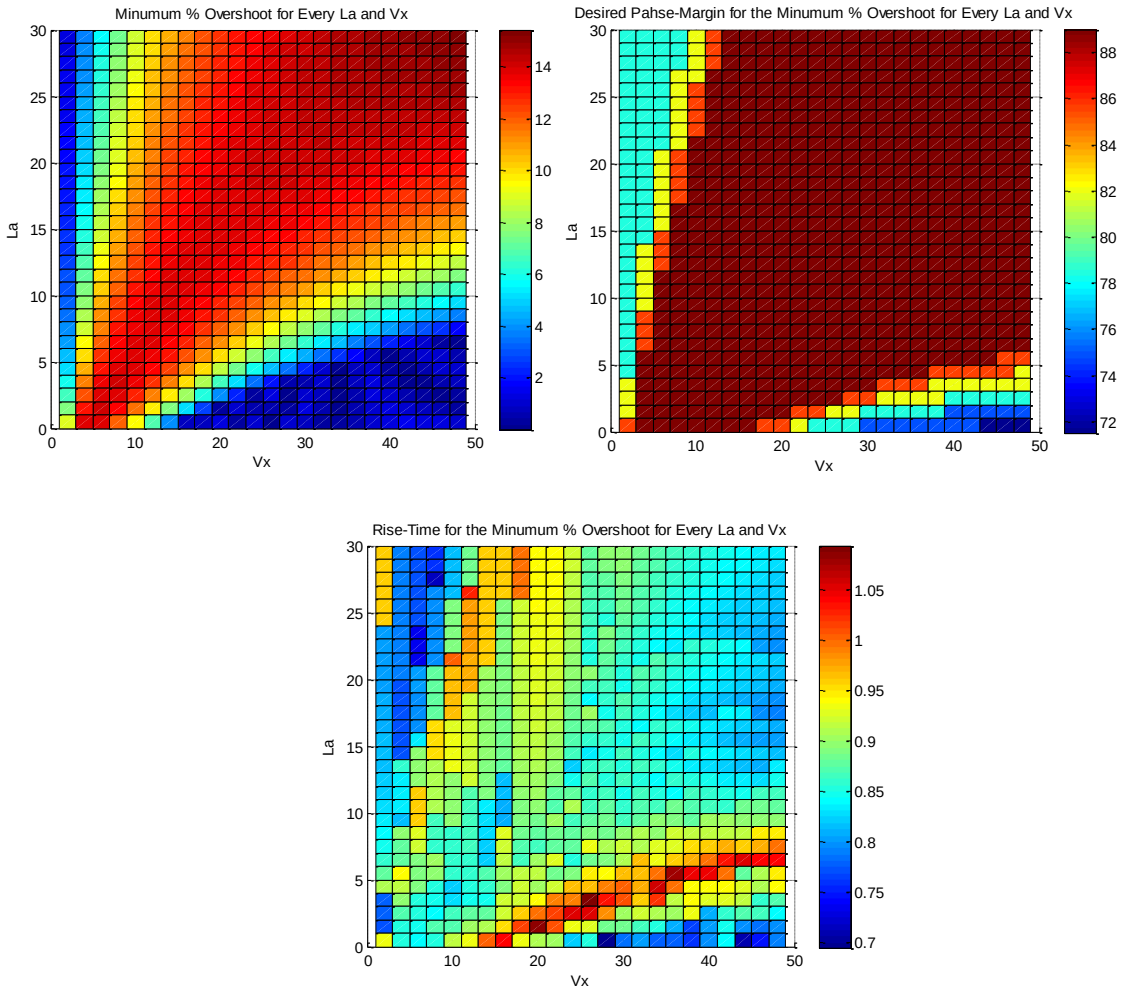

Figures 7.2.4-7.2.6: Plots of minimum overshoot, its associated phase-margin and rise-time, respectively for a crossover frequency of 2rad/s.

Next, some typical step responses associated with achieving minimum overshoot is of interest and is shown in the figures below.

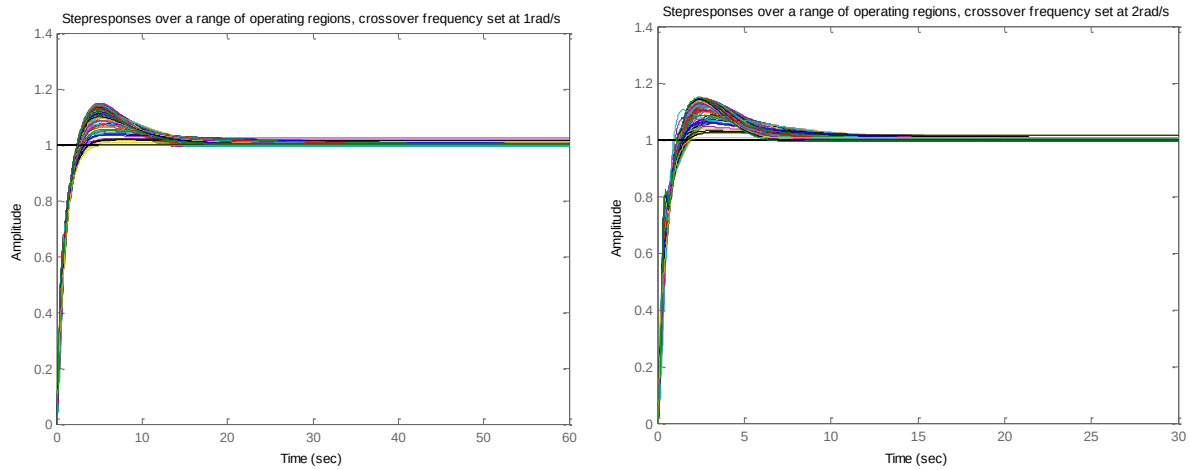

Figures 7.2.7-7.2.8: Plots of the step responses that achieve minimum overshoot, for crossover frequencies of 1rad/s and 2rad/s respectively.

As can be seen from the figures above, it is possible with a PD-controller to achieve relatively low overshoot for the desired operating areas, i.e. high speeds and low look-ahead distances. Furthermore, by selection of the crossover frequency, these minimum overshoots could be achieved while maintaining the desired rise-time of about 1 second. However, as mentioned in the beginning of Section 5 it is also desired that the system maintains a reasonable settling-time, and from what can be seen from the step-responses, the settling-time is rather high and it manifests itself similar to a slowly dissipating steady-state error. Thus, tuning the controller to maintain a minimum overshoot presents the drawback of having long settling-time.

Since it is also desired to maintain a fixed rise time, the following plots show the associated overshoot and phase margins with fixing the rise-time to one second. Since it is not possible to maintain the same rise time for every operating point, the best results with rise time within 20% of the desired one are selected. In case no point exists within the 20% range, those points are set to zero in the plotted data and would appear as dark blue squares.

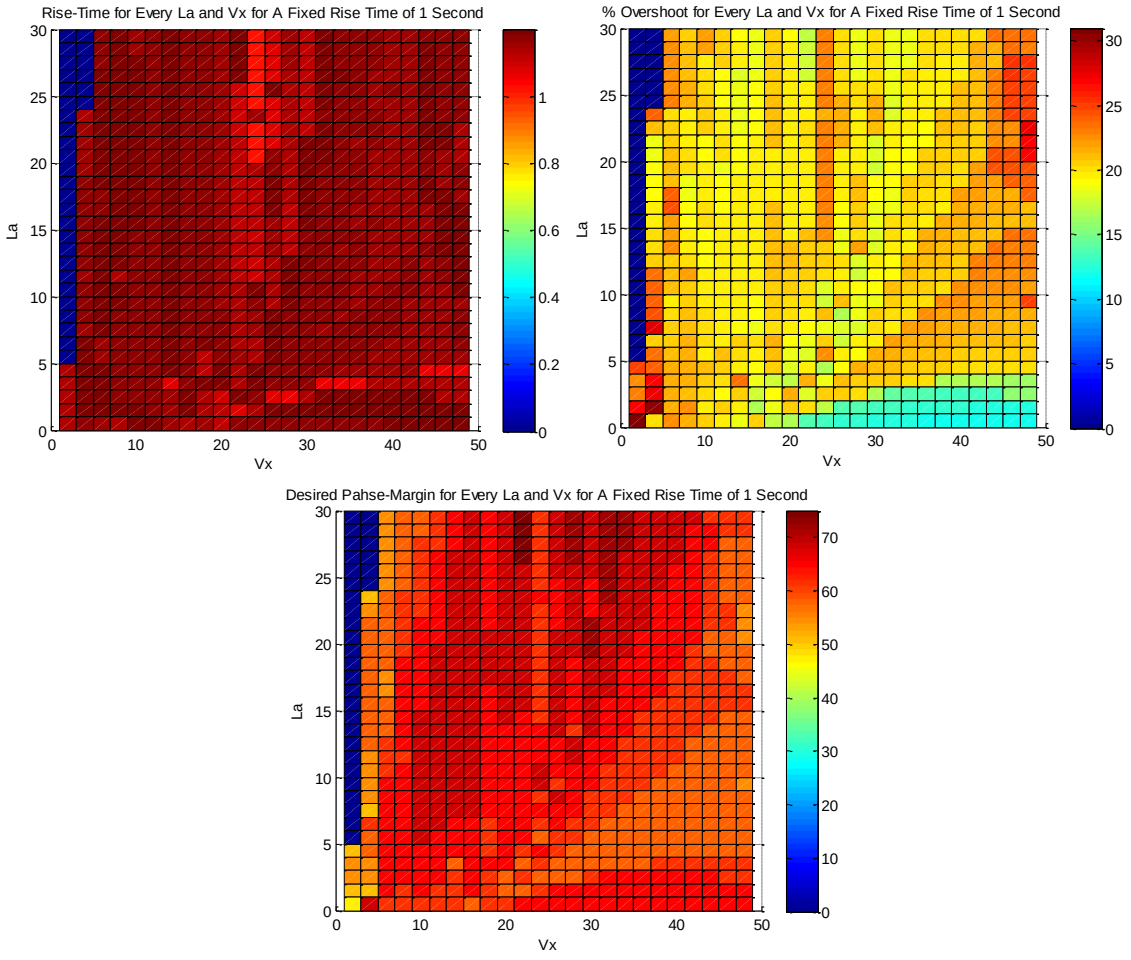

Figures 7.2.9-7.2.11: Plots of chosen rise-time, its associated over-shoot and phase-margin, respectively for a crossover frequency of 1rad/s.

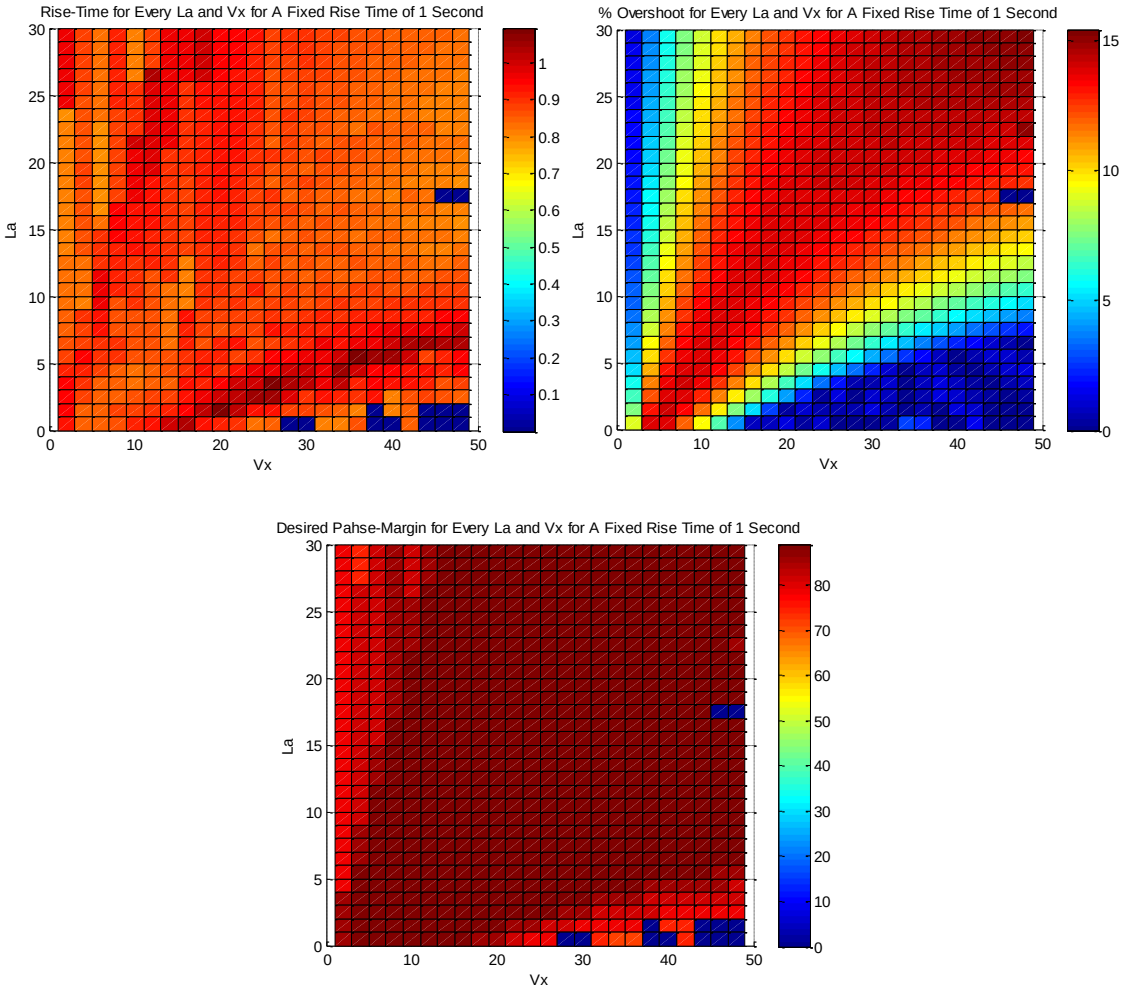

Figures 7.2.12-7.2.14: Plots of chosen rise-time, its associated over-shoot and phase-margin, respectively for a crossover frequency of 2rad/s.

Similar to before, typical step responses associated with achieving a fixed rise-time of about one second and the control signals requested are also of interest and are shown in the figures below.

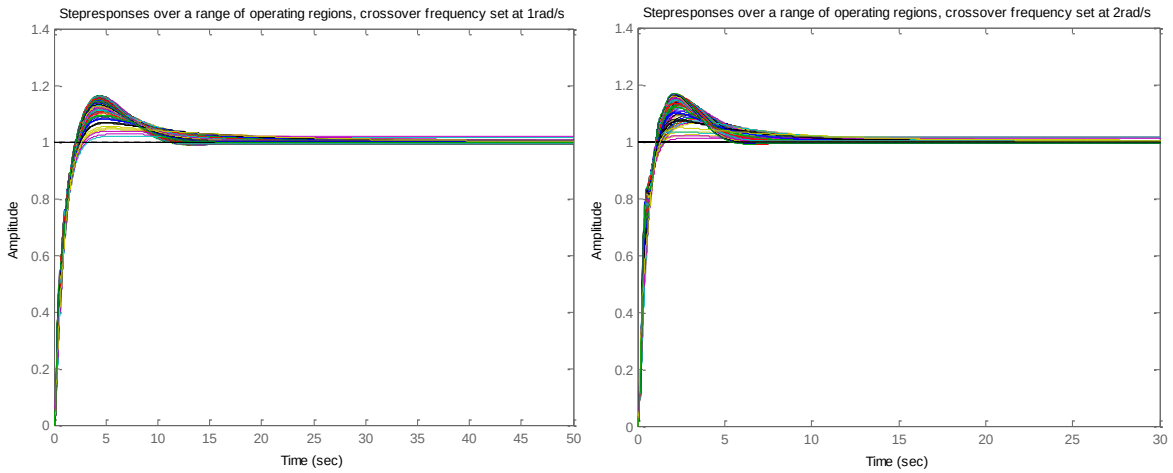

Figures 7.2.15-7.2.16: Plots of the step responses that achieve a fixed rise-time of about 1 second, for crossover frequencies of 1rad/s and 2rad/s respectively.

The figures above show that if having the criteria to maintain a fixed rise-time, larger overshoot than in the previous case will be present. However, the settling-time will be considerably lower for the cases where the overshoot is not minimized as some of them have a rise time of about 1 second. Thus, it can be concluded that, for this system and this set-up, one of the criteria mentioned in Section 5, must be violated in order for the other two to hold.

The two figures below present the maximum overshoot that may occur using this controller for the settings mentioned in the beginning, to visualize the worst-case scenario during tuning.

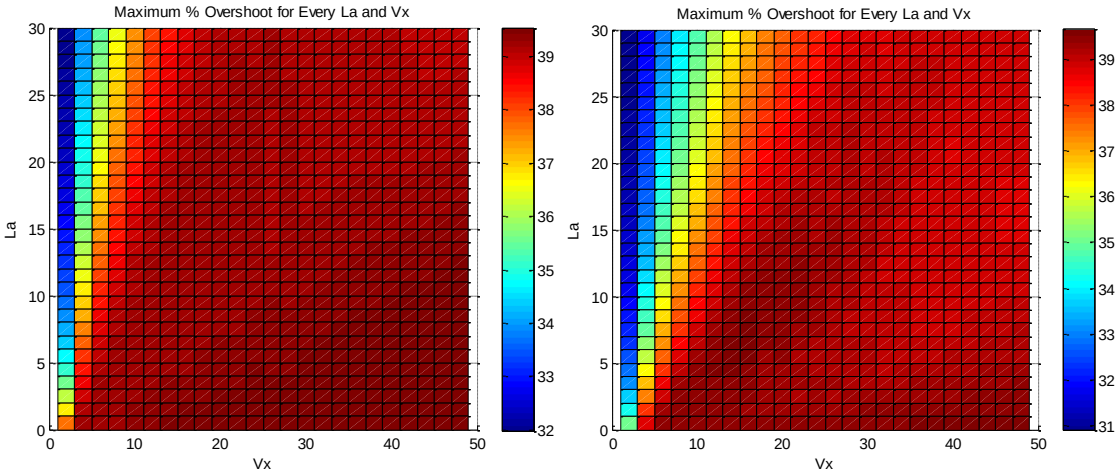

Figures 7.2.17-7.2.18: Plots of maximum over-shoot over all operating range for a crossover frequency of 1rad/s and 2rad/s respectively.

7.3 PDD-Controller

For the design parameters mentioned for the PD case, similar analysis is done using the tuning rule defined in Section 5.2. First, the following plots show the minimum overshoot achieved for a given crossover frequency and the phase margins under which they are achieved at along with the rise-time for the responses.

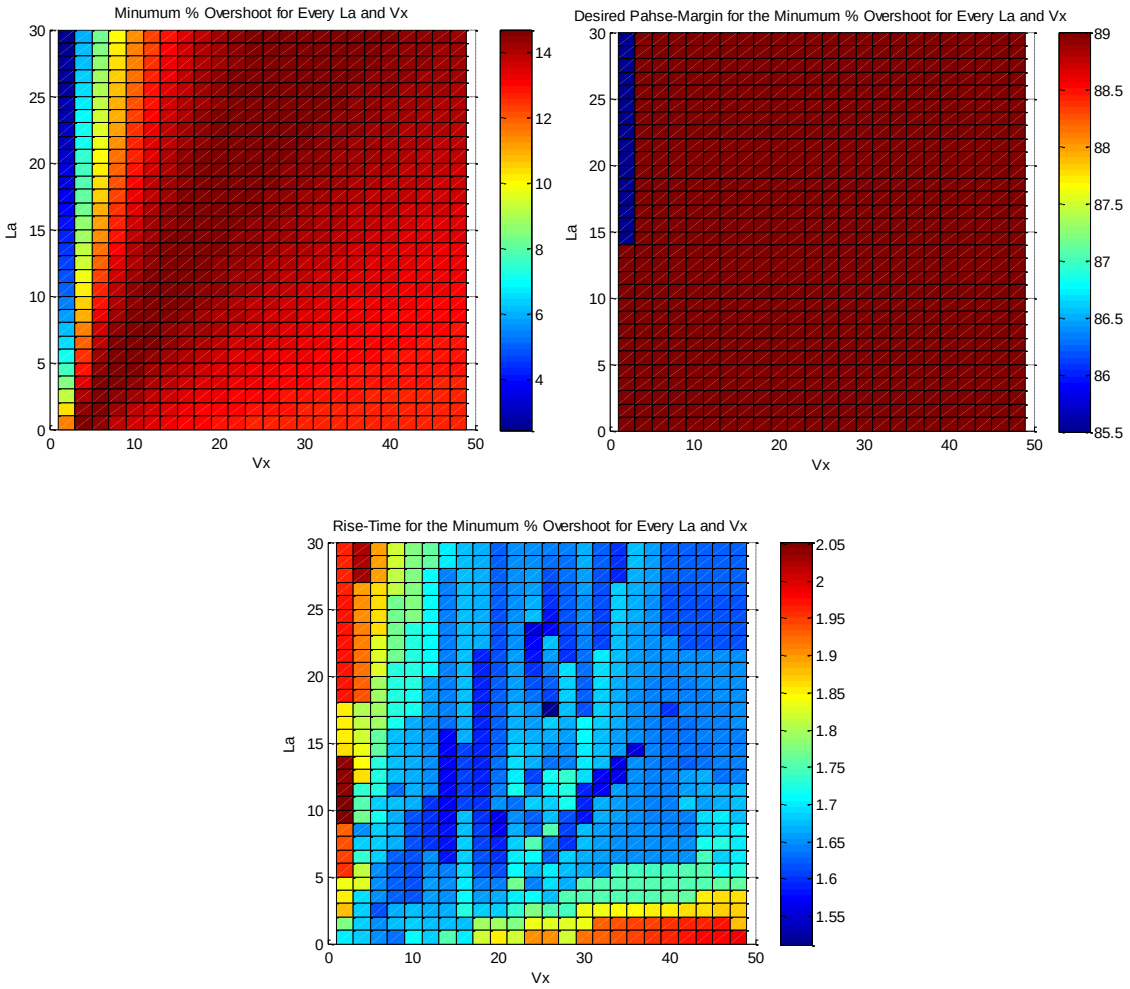

Figures 7.3.1-7.3.3: Plots of minimum overshoot, its associated phase-margin and rise-time, respectively for a crossover frequency of 1rad/s.

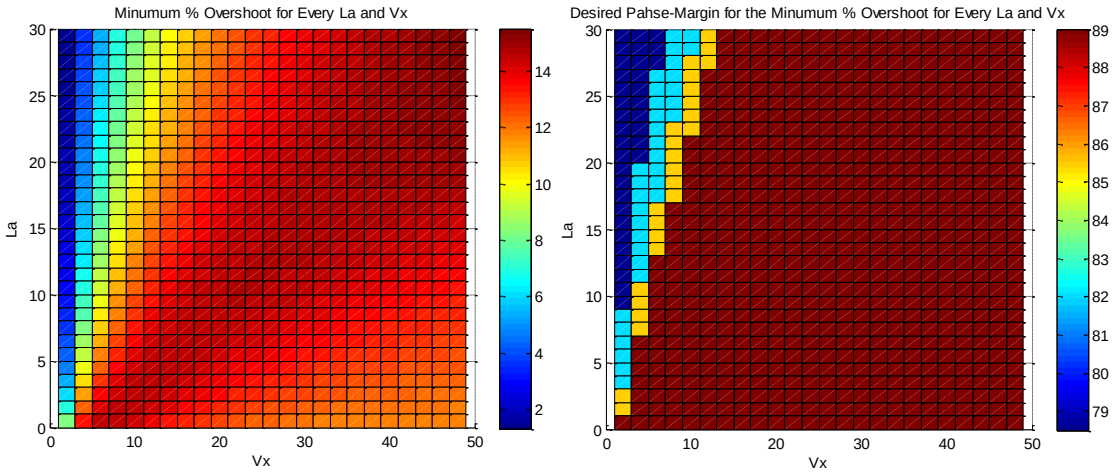

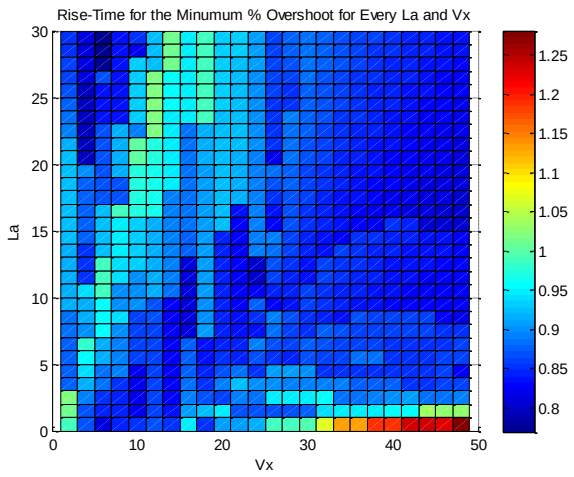

Figures 7.3.4-7.3.6: Plots of minimum overshoot, its associated phase-margin and rise-time, respectively for a crossover frequency of 2rad/s.

Similar to the PD case, it is also desired to look at some typical step responses associated with achieving minimum overshoot and the control signals requested. They are shown in the figures below.

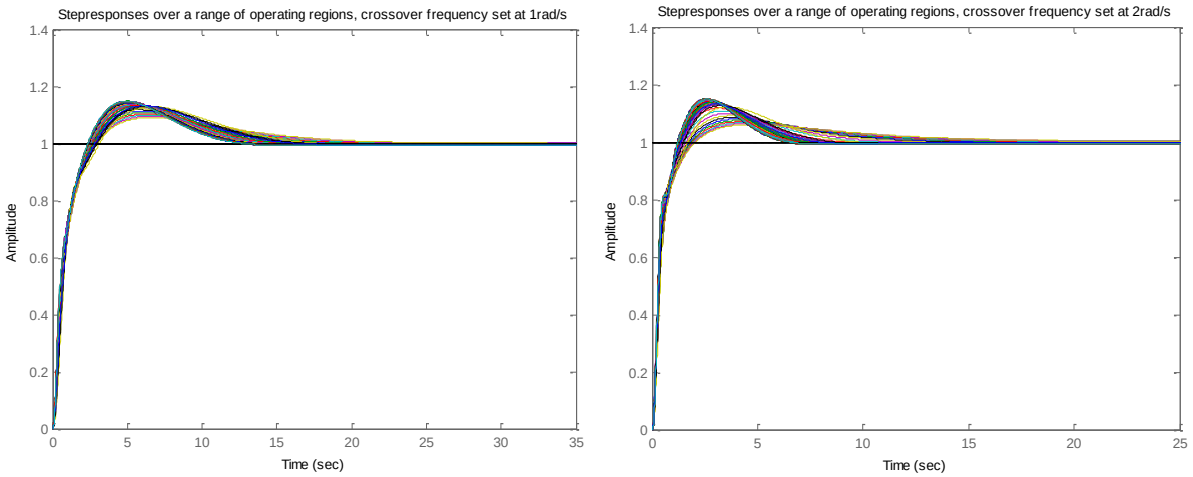

Figures 7.3.7-7.3.8: Plots of the step responses that achieve minimum overshoot, for crossover frequencies of 1rad/s and 2rad/s respectively.

The figures above show similar characteristics to the PD-controller case. However, one difference that can be noted is that minimum overshoot is not attained in the same in the same area as in the previous case, using this tuning rule. Furthermore, using this controller yields a somewhat faster settling-time.

Next, for a fixed rise-time within a 20% limit, the following results are obtained.

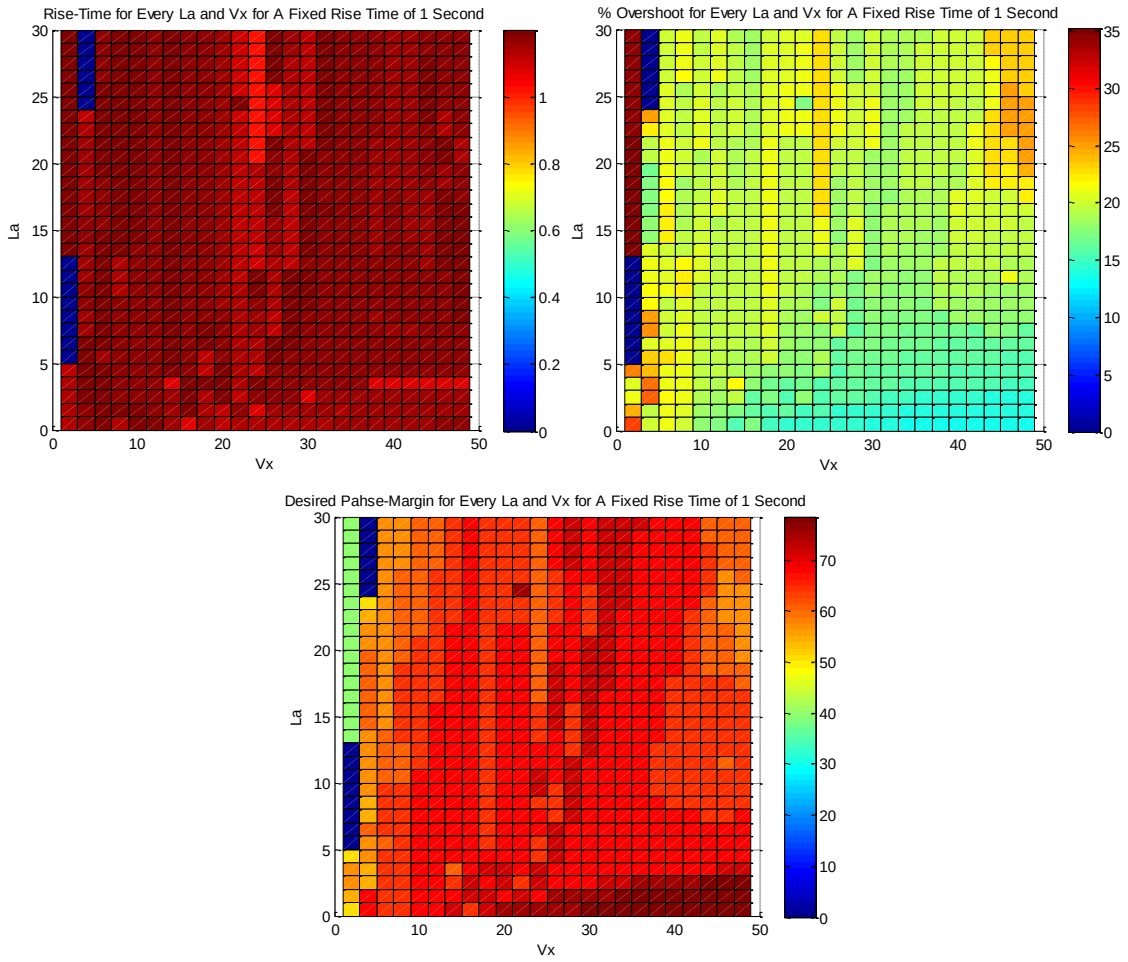

Figures 7.3.9-7.3.11: Plots of chosen rise-time, its associated over-shoot and phase-margin, respectively for a crossover frequency of 1rad/s.

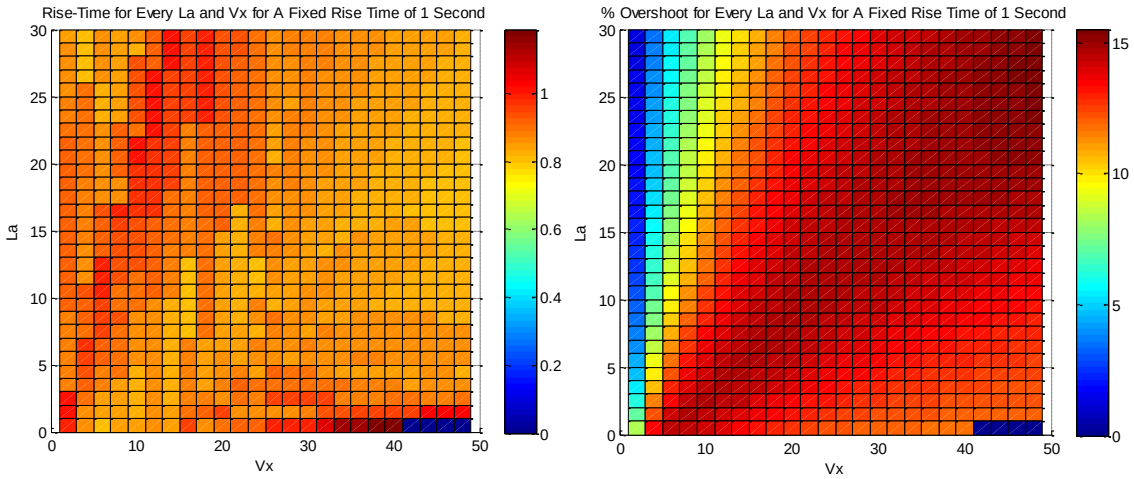

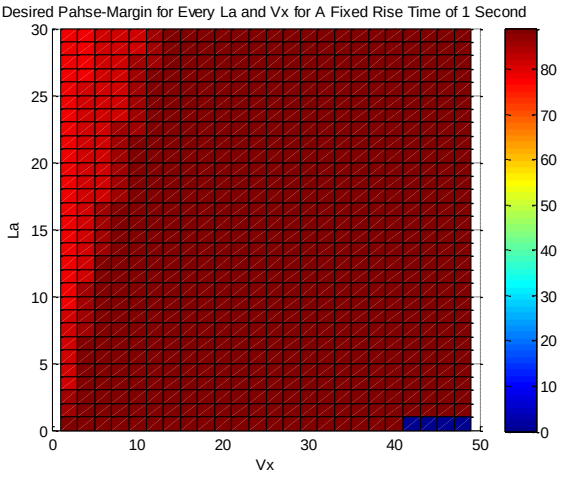

Figures 7.3.12-7.3.14: Plots of chosen rise-time, its associated over-shoot and phase-margin, respectively for a crossover frequency of 2rad/s.

Similar to before, a look at some typical step responses associated with achieving a fixed rise-time of about one second and the control signals requested is also of interest and is shown in the figures below.

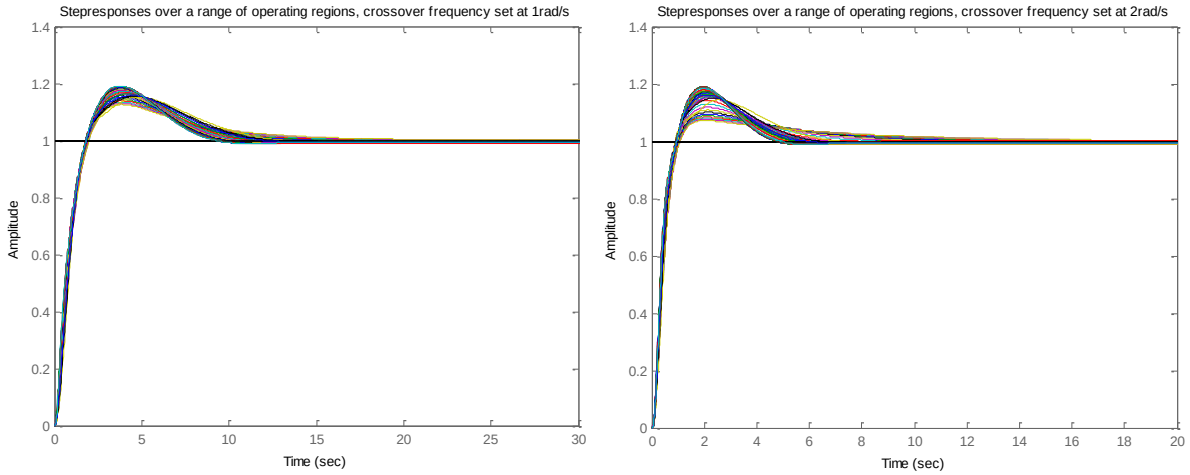

Figures 7.3.15-7.3.16: Plots of the step responses that achieve a fixed rise-time of about 1 second, for crossover frequencies of 1rad/s and 2rad/s respectively.

The results above show similarity to the ones obtained with the PD-controller. However, once again, shorter settling-time is noted.

The two figures below present the maximum overshoot that may occur using this controller for the settings mentioned in the beginning and the tuning rule in Section 5.2, to visualize the worst-case scenario during tuning.

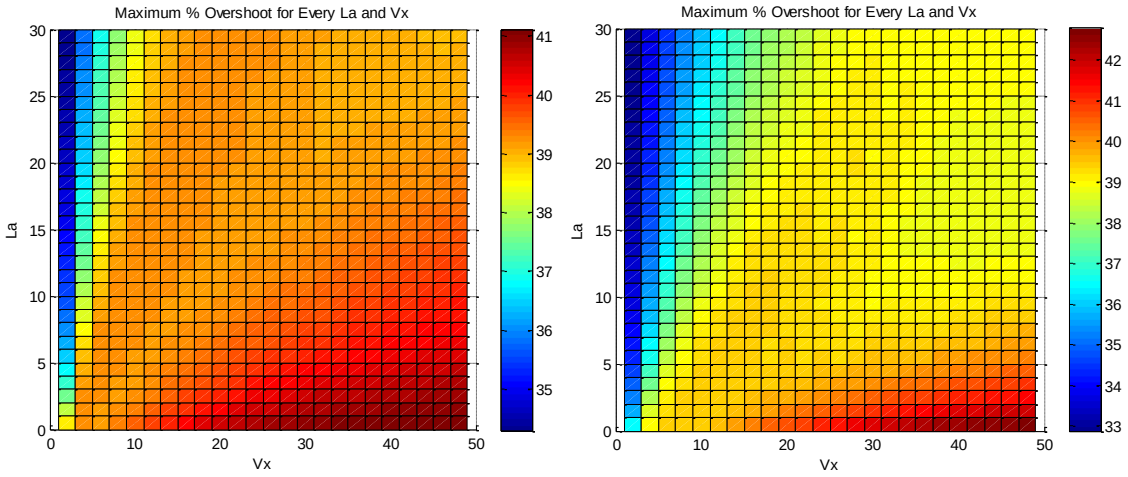

Figures 7.3.17-7.3.18: Plots of maximum over-shoot over all operating range for a crossover frequency of 1rad/s and 2rad/s respectively.

7.4 Pole-Placement Design

Using the rules specified in Section 5.3 for placing the poles, will for each velocity between 10m/s and 30m/s, over a range of look-ahead distances from 1m to 15m, result in a maximum of 37% overshoot and a minimum of 13%, while the rise-time is kept between roughly 0.5s to 1.5s (the faster rise-times belonging to higher velocities).

The figures 7.4.1-7.4.6 below show the step-responses of the closed-loop system, including actuator, for some velocities and look-ahead distances.

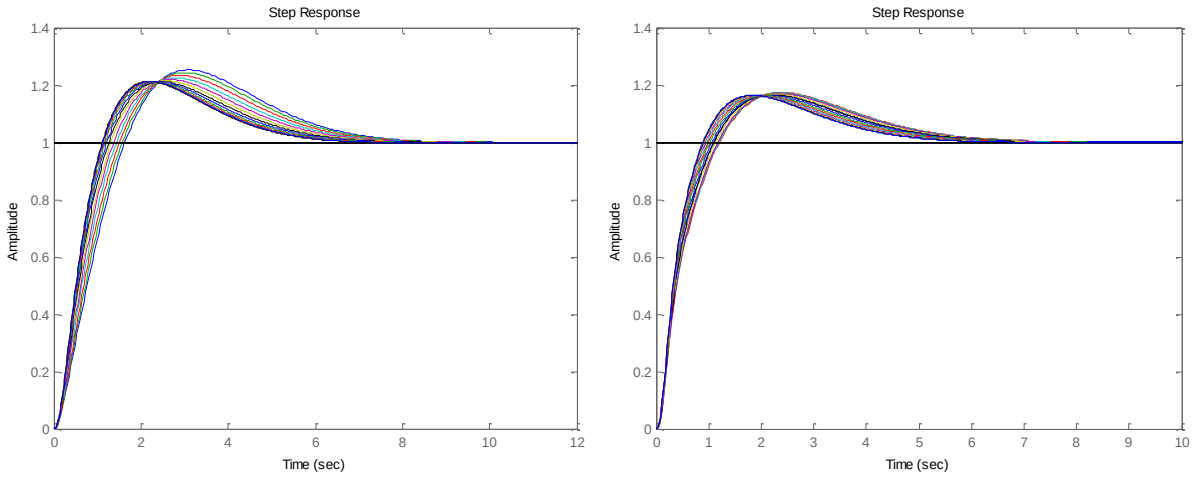

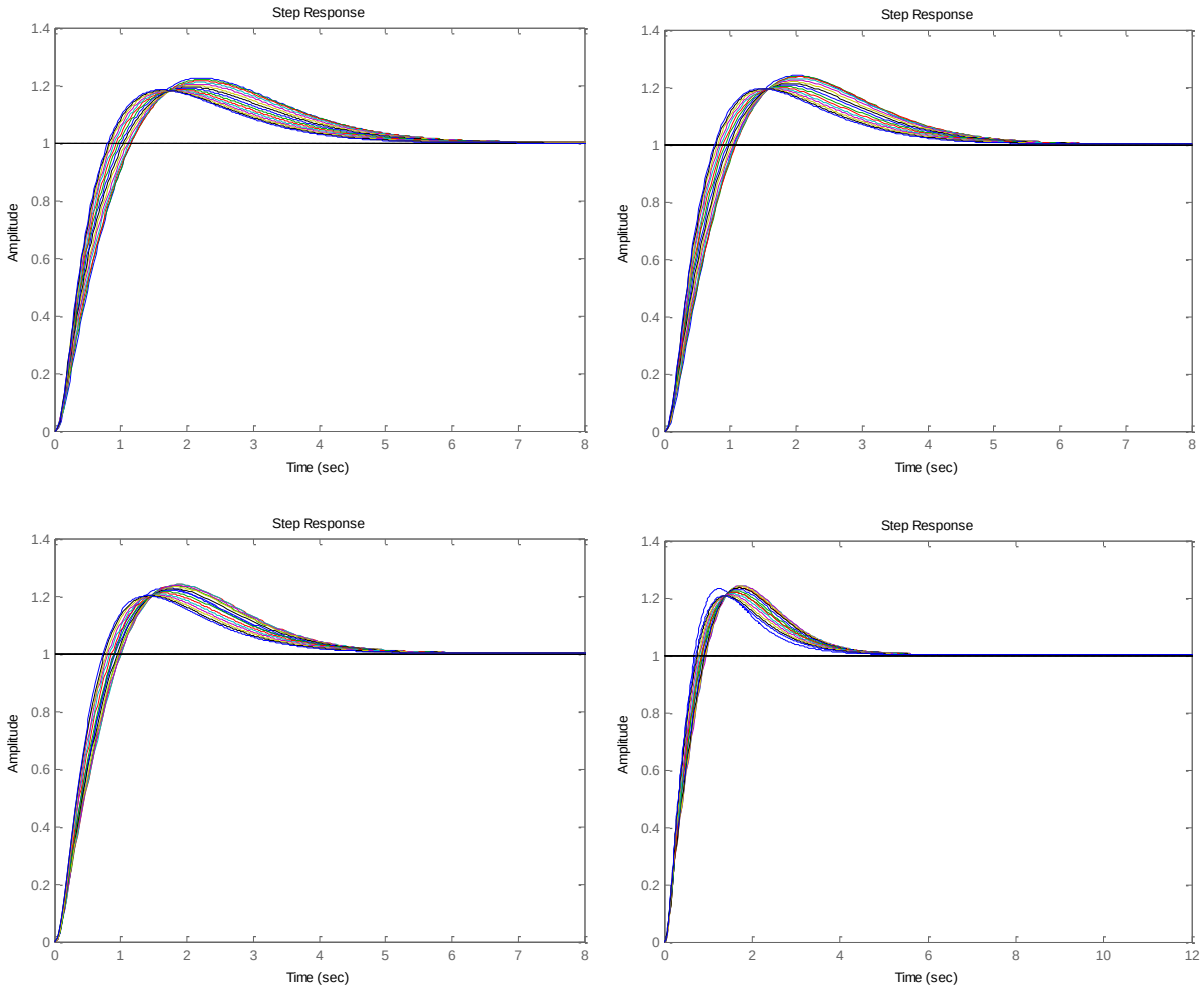

Figures 7.4.1-7.4.6: Step-responses of closed-loop system with actuator included. Each figure is for a set velocity of 10, 14, 18, 22, 26 and 30m/s respectively, displaying look-ahead distances ranging from 1m to 15m

At each velocity, the responses are rather similar regardless of the amount of look-ahead. Although it is apparent that it is possible to achieve acceptable behaviour and consistency to some extent even when excluding the look-ahead distance from the tuning rules, using the same controller for a large range of velocities and look-ahead distances presents issues. As an example, at velocities less than 10m/s when including the actuator the system would be unstable. In contrast to the previous two approaches, this method presents rather fast settling-time.

7.5 Control signals

In this part, the control signals for selected tuning rules are displayed. This is to ensure that the tuning rules do not output unreasonable signals to the actuator.

7.5.1 PD-Controller

The parameters tuned are $\omega_c = 1$ and $\phi_m = 85$ for the minimum overshoot requirement. The plotted data are for speeds between 20-40 m/s and look-ahead distances from 0-5m

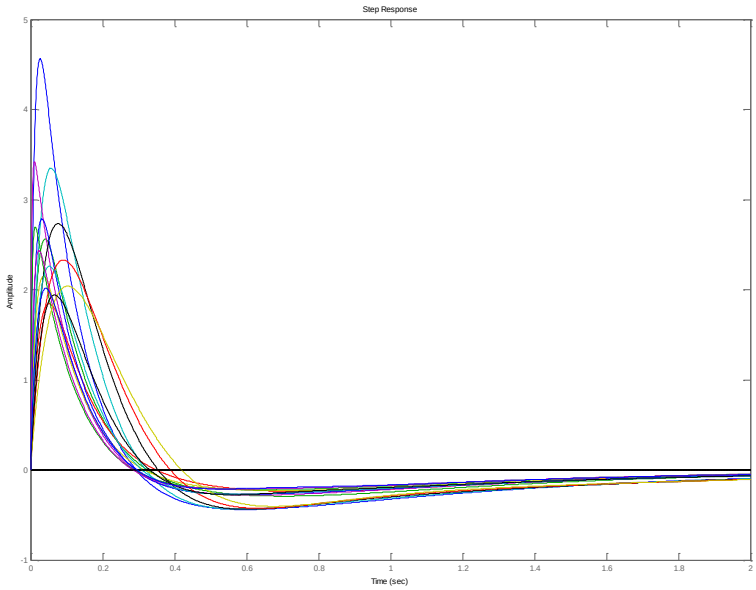

Figure 7.5.1.1: Control signal for PD-controller with crossover frequency of 1rad/s and phase margin of 85 degrees. Speeds and look-ahead distances varied as specified above.

As can be seen, no more that 4.5 degrees in the worst case are requested from the actuator and the control signals are smooth.

In the case where $\omega_c = 2$ and $\phi_m = 76$ for minimum overshoot.

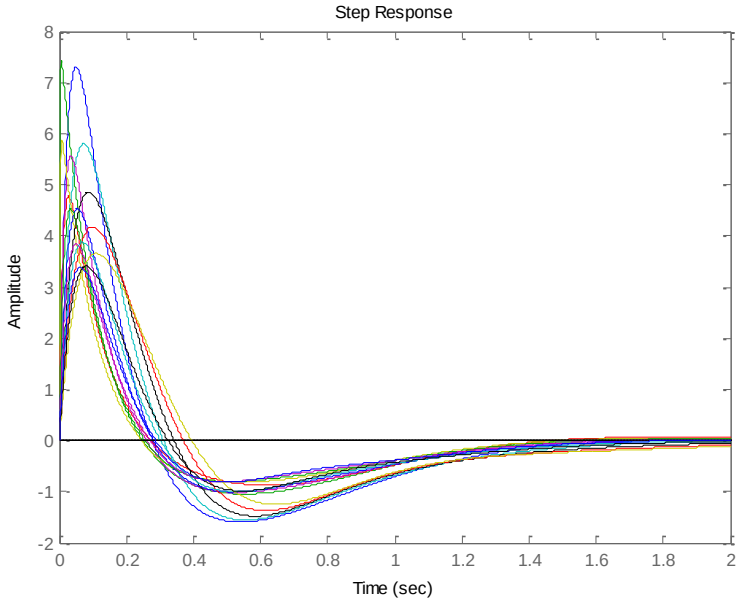

Figure 7.5.1.2: Control signal for PD-controller with crossover frequency of 2rad/s and phase margin of 76 degrees. Speeds and look-ahead distances varied as specified above.

As can be seen, in the two cases the system achieves almost similar overshoots but in the case where $\omega_c = 2$ the response of the system is much faster. That results in the control signal having increased in magnitude compared to the previous case.

7.5.2 PDD-Controller

Similar to the PD case, the plots of the input signals are shown below

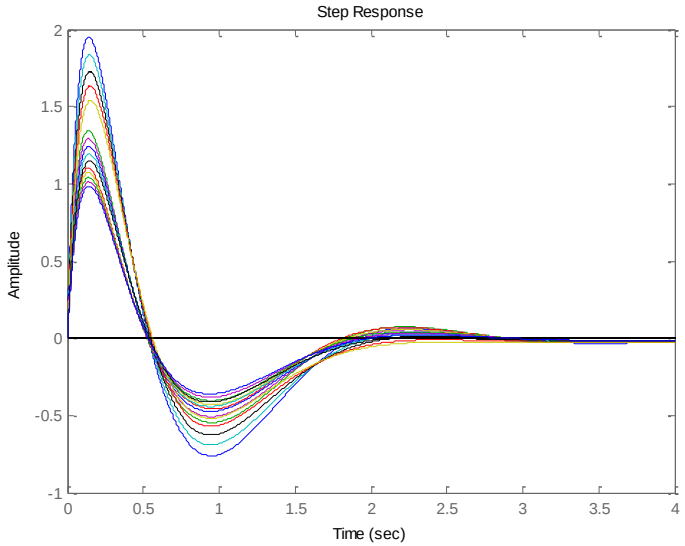

Figure 7.5.2.1: Control signal for PDD-controller with crossover frequency of 1rad/s and phase margin of 89 degrees. Speeds and look-ahead distances varied as specified above.

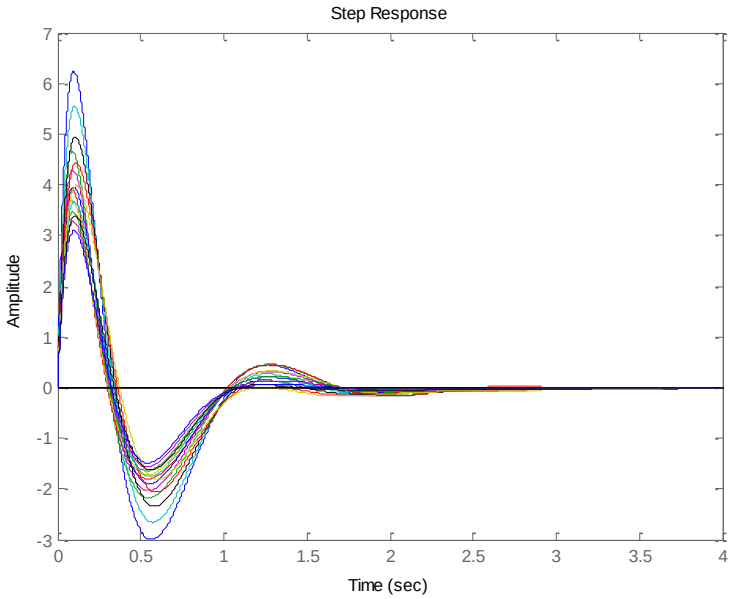

Figure 7.5.2.2: Control signal for PDD-controller with crossover frequency of 2rad/s and phase margin of 89 degrees. Speeds and look-ahead distances varied as specified above.

It can be noted that this method requires less control action when compared to the PD-controller.

7.5.3 Pole-Placement Design

The control signals for velocities ranging from 20-30m/s and look-ahead distances from 1m to 5m are shown below, for the tuning rules specified in Section 5.3.

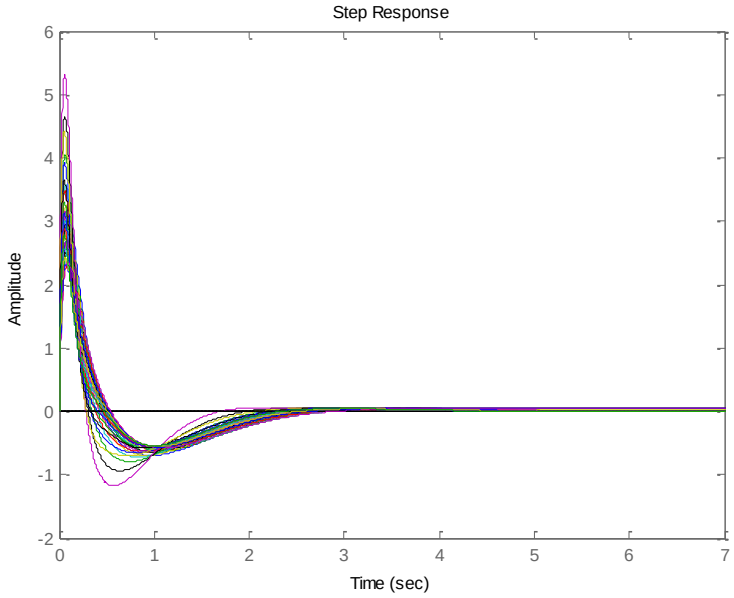

Figure 7.5.3.1: Control signal for Pole-Placement Design with velocities and look-ahead distances ranging as specified above.

As can be seen from the figure above, the controller does ask for unreasonable signals from the vehicle and is within the same range as the other controllers discussed above.

7.6 String Stability

Before presenting the results from the topologies discussed, it is of interest to see why the topology introduced in Section 6.3.2 was abandoned. Since the aim is to have a platoon moving at high velocities and short look-ahead distances, the following figure shows the magnitude of the ratio of the lateral error of the fourth follower to the third follower for velocities between 15m/s and 40m/s and look-ahead distances ranging from 1.54m to 11.54m. The controller is a PD chosen to maintain a crossover frequency of 1rad/s and a desired phase margin of 50 degrees with the absolute look-ahead distance (from bumper to bumper) chosen at the discrete values $L_a = [1\ 4\ 7\ 10]$m.

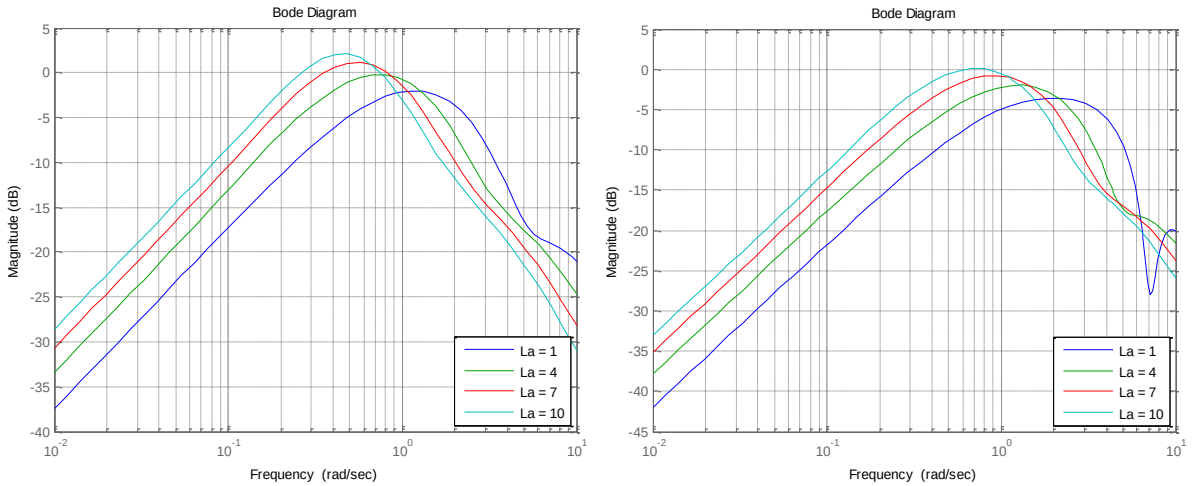

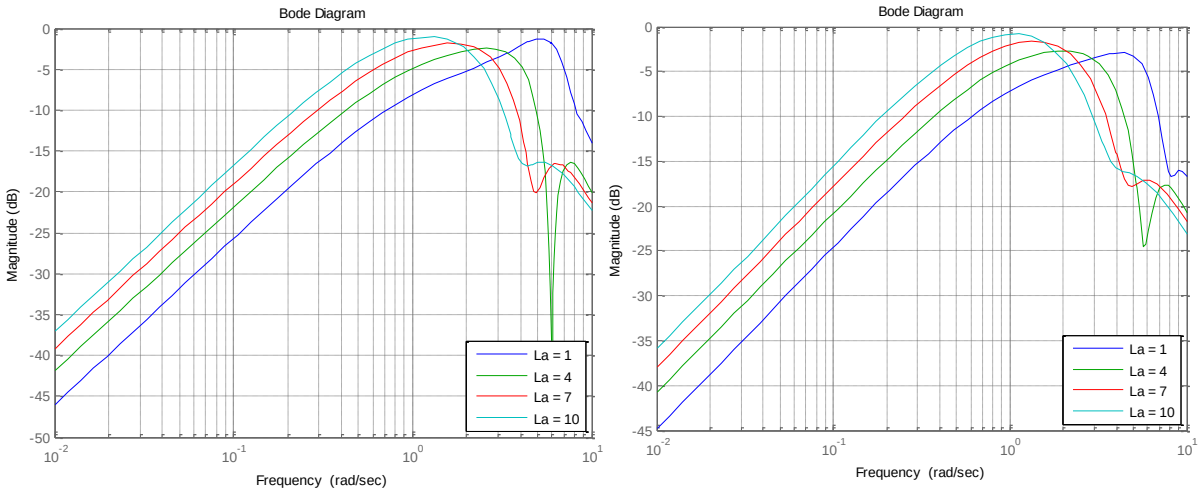

Figures 7.6.1-7.6.4: *The ratio of error for look-ahead distances ranging from 1 to 10 for a fixed velocity of 15m/s, 25m/s, 35m/s and 40m/s respectively.*

As can be seen, the ratio is dependent on the operating condition of the platoon. However, maintaining a look-ahead distance less that 4m would guarantee string stability up until the fourth follower under all operating points evaluated.

A note should be made on the selection of the constant k. Let k be selected to -1, thus, starting from follower 2 and substituting k in (6.3.2.10)

$$\varepsilon_2 = \frac{G_{rb}C(-1+1)}{(1+G_{\Delta y}C)}\varepsilon_1 = 0\ \forall\omega \tag{7.6.1}$$

This basically means that the second follower anticipates the first follower's movements and moves accordingly and hence achieves perfect following. Moving to the third follower's expression in (6.3.2.13)

$$\varepsilon_3 = \frac{G_{rb}C\left(-\left(\frac{A_{rb}}{A_{\Delta y}}\right)+1\right)}{(1+G_{\Delta y}C)}\varepsilon_2 = \frac{G_{rb}C\left(-\left(\frac{A_{rb}}{A_{\Delta y}}\right)+1\right)}{(1+G_{\Delta y}C)} * (0) = 0\ \forall\omega \tag{7.6.2}$$

and similarly for the vehicles further down the platoon. This means that the vehicles in the platoon will move in synchronization as soon as the first follower has a deviation from the leader. This can be seen from the following figure where the movement of a platoon of six followers is shown when a disturbance is given to the leader's position.

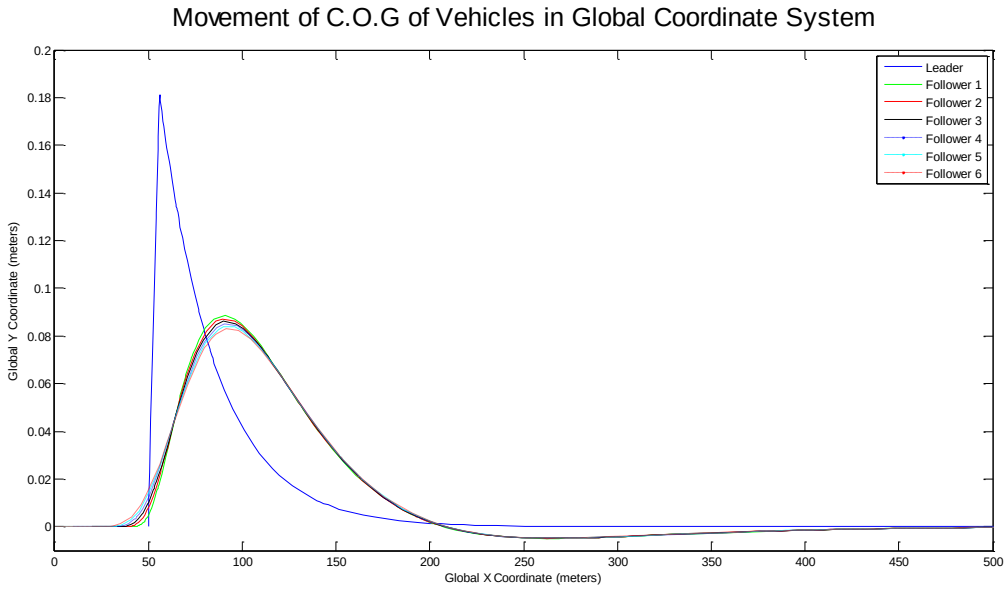

Figures 7.6.5: *Simulation results of the movements of a platoon of six followers when a disturbance is given to the leader for 30m/s velocity and 7.54m look-ahead distance.*

As can be seen, all followers from the second onwards follow the first follower and it was observed that each has zero lateral deviation to the vehicle in front of it. This, however, does not mean that the platoon is string stable. As can be seen from figures 7.6.1-7.6.4, if a disturbance is introduced from the third follower to the fourth at the frequencies where the amplitude of the norm is greater than one, that error will increase in magnitude for the fourth follower. Hence, this platoon of six followers is not string stable. This shows the necessity to look at the explicit expression as in (6.3.2.16) for every index i and show how the infinity norm is always kept strictly less than one.

Thus, the focus of the remainder of the chapter will be on the remaining topologies.

For the different communication topologies presented in Section 6, a number of simulations were done with a platoon of 17 vehicles. There are two main cases that are simulated. The first is that the platoon will move in a straight trajectory, while a disturbance acts on the second following vehicle at some point in time. The other case is that the second follower will get that same disturbance while the platoon is performing a lane change manoeuvre. The interest would lie in observing how this error will propagate in the platoon starting from the third follower. In the two following cases, a PD-controller was used with a set-up of crossover frequency of 1rad/s and a phase-margin of 60 degrees, while the platoon was moving with a velocity of 30m/s with a look-ahead distance of 1.5m. The feed-forward filter F was in topologies 1 and 2 chosen to be $-0.5C\frac{A_{rb}}{A_{\Delta y}}$; for the settings of the remaining topologies, please refer to Patent I2828SE00. For the sake of simplification, the communication topology described in Section 6.2 will be called *topology 1*, the one in Section 6.3.1 *topology 2*, the ones described in Patent I2828SE00 will be called *topology 3* and *topology 4* respectively.

7.6.1 Case 1: Disturbance While on a Straight Trajectory

The plots below illustrate the maximum of the absolute lateral error relative to the preceeding vehicle as a function of vehicle number in the platoon for the four topologies introduced in Section 6.

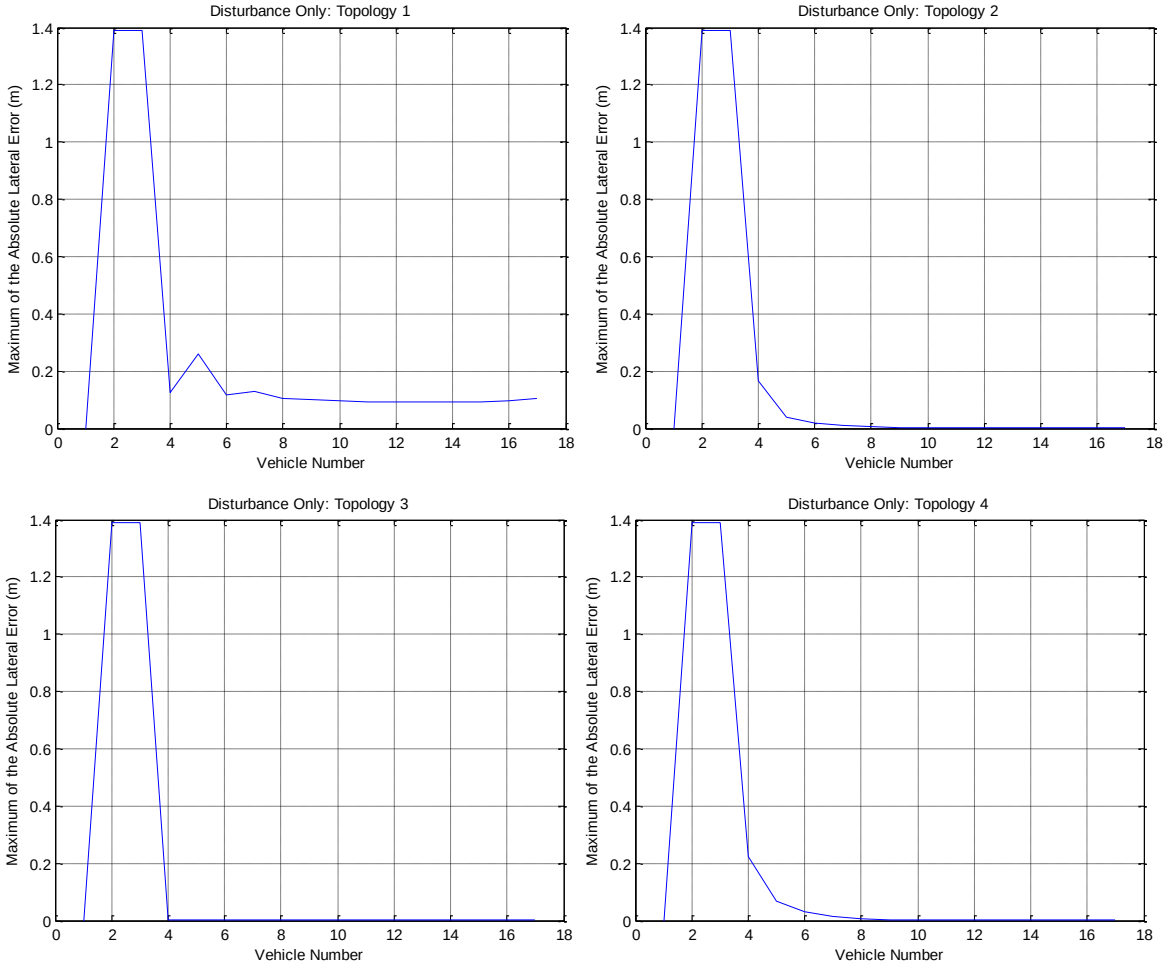

Figures 7.6.1.1-7.6.1.4: *Maximum of the absolute lateral error for a platoon of seventeen followers when a disturbance is given to the second follower.*

As can be seen from the first figure in the above set, by using topology 1, that is having information from only the preceding vehicle, makes the platoon string unstable. However, the other three methods clearly resolve in a string stable platoon, as the error attenuates and reaches 0. Comparing topology 3 and topology 4, it can be seen that in the latter case there is control over the rate of dissipation of the error. It is to be noted, although topology 2 presents a string stable platoon, it has been assumed that the vehicles move with no yaw.

It is also of interest to look at the maximum steering wheel angle performed by each follower. The following figures show that kind of information.

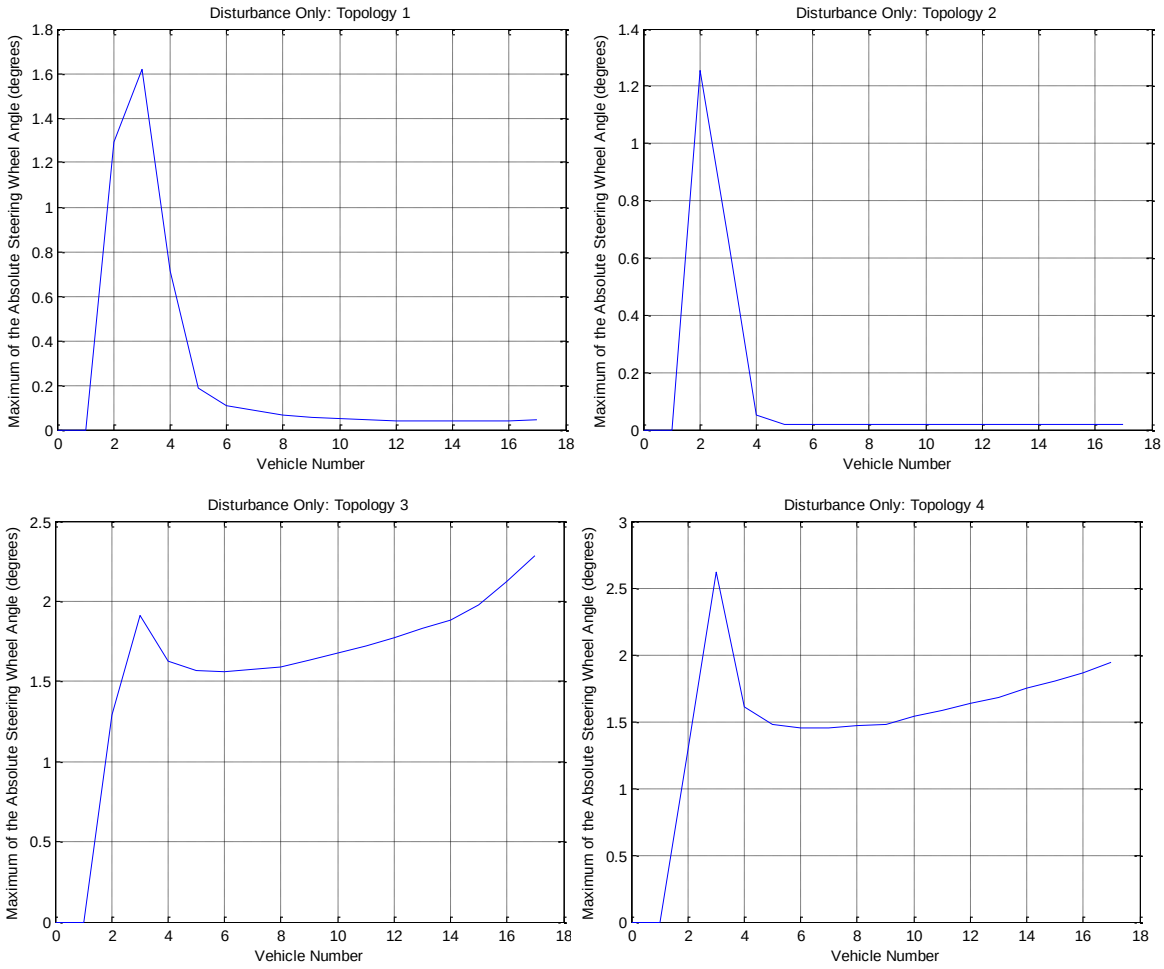

Figures 7.6.1.5-7.6.1.8: *Maximum control signal requested for a platoon of seventeen followers when a disturbance is given to the second follower.*

As can be seen, the two latter topologies require larger control signals in order to keep the platoon string stable. Furthermore, it can be noted that the demand on the steering-wheel angle is increasing for vehicles further down the platoon, although not at a very high rate. The absolute maximum is less than 2.7 degrees.

7.6.2 Case 2: Disturbance While Performing a Lane Change

Similar to the previous case, the plots below illustrate the maximum of the absolute lateral error as a function of each vehicle in the platoon for the four topologies introduced in Section 6.

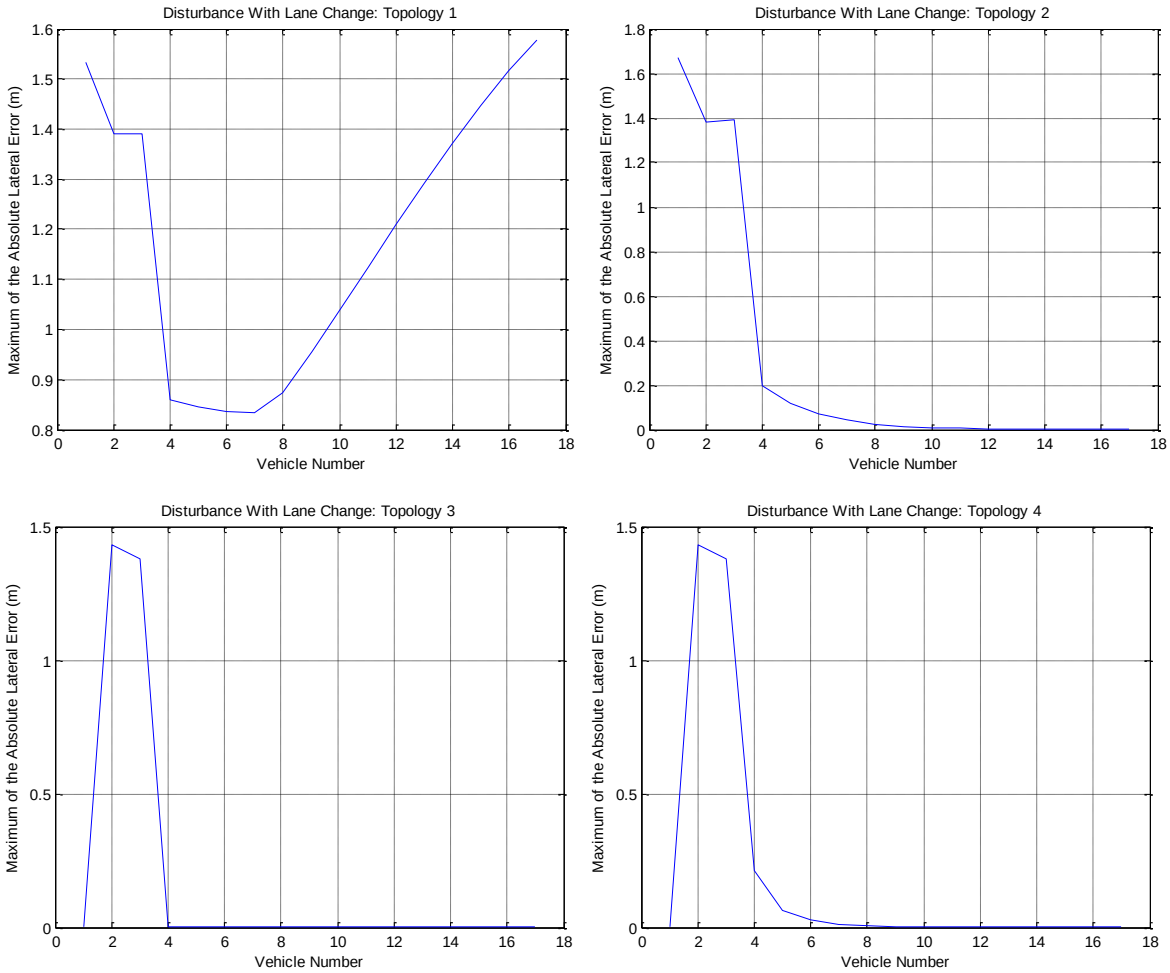

Figures 7.6.2.1-7.6.2.4: *Maximum of the absolute lateral error for a platoon of seventeen followers when a disturbance is given to the second follower while the leader is performing a lane change manoeuvre.*

Similarly, for this kind of manoeuvre, the same conclusions can be drawn about string stability as in the previous case. However, it has to be noted that the latter two topologies require a larger maximum control signal, as can be seen in the following plots.

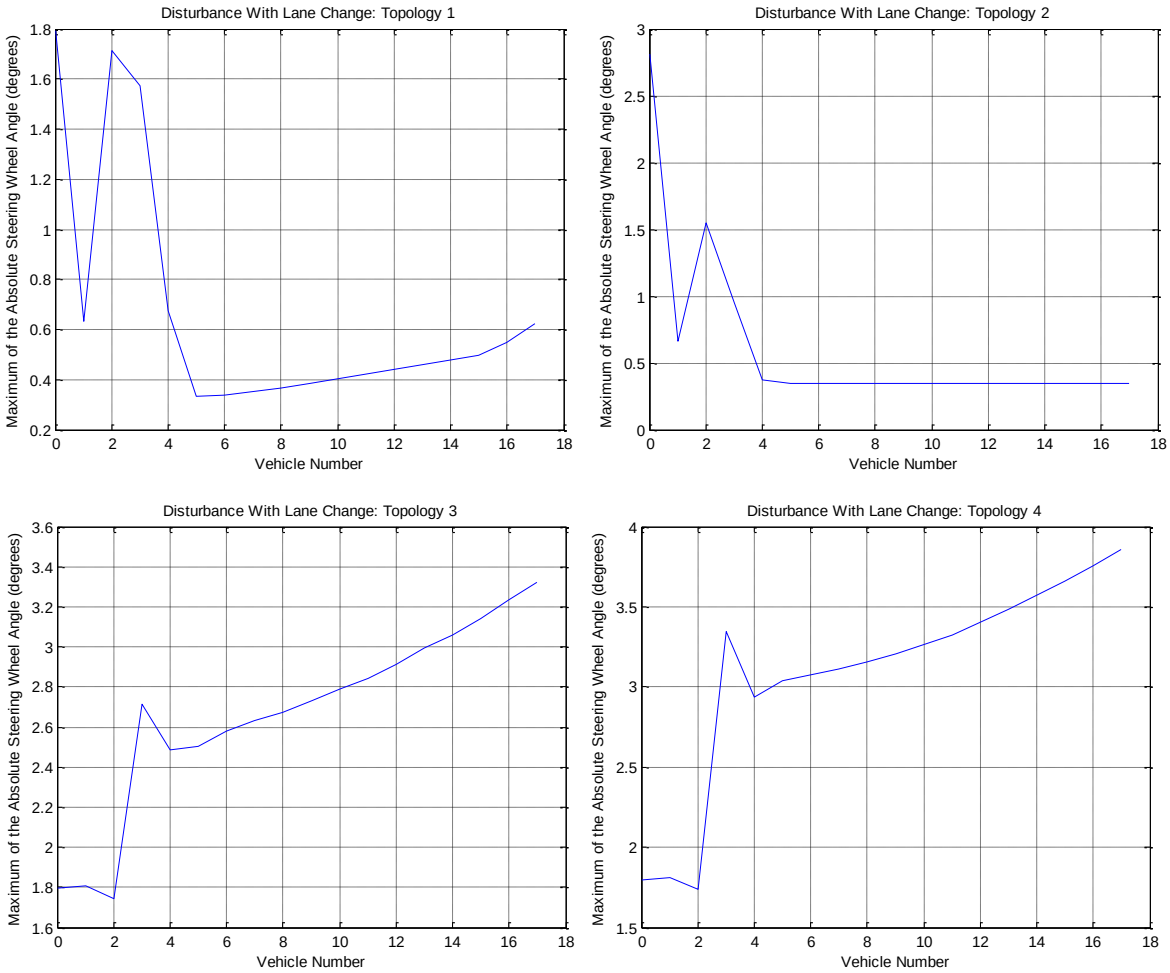

Figures 7.6.2.5-7.6.2.8: *Maximum control signal requested for a platoon of seventeen followers when a disturbance is given to the second follower while the leader is performing a lane change manoeuvre.*

7.6.3 In Case of Model Uncertainties

In the previous cases, perfect knowledge on the parameters of vehicles involved in the platoon guaranteed string stability to an infinite number of vehicles. Thus, the results of the effect that model uncertainties have on the number of vehicles in a platoon that can be guaranteed to be string stable is shown below. The simulation was conducted with the PD-controller described in Section 5.1, with a crossover frequency of 0.5rad/s and a phase-margin of 45 degrees.

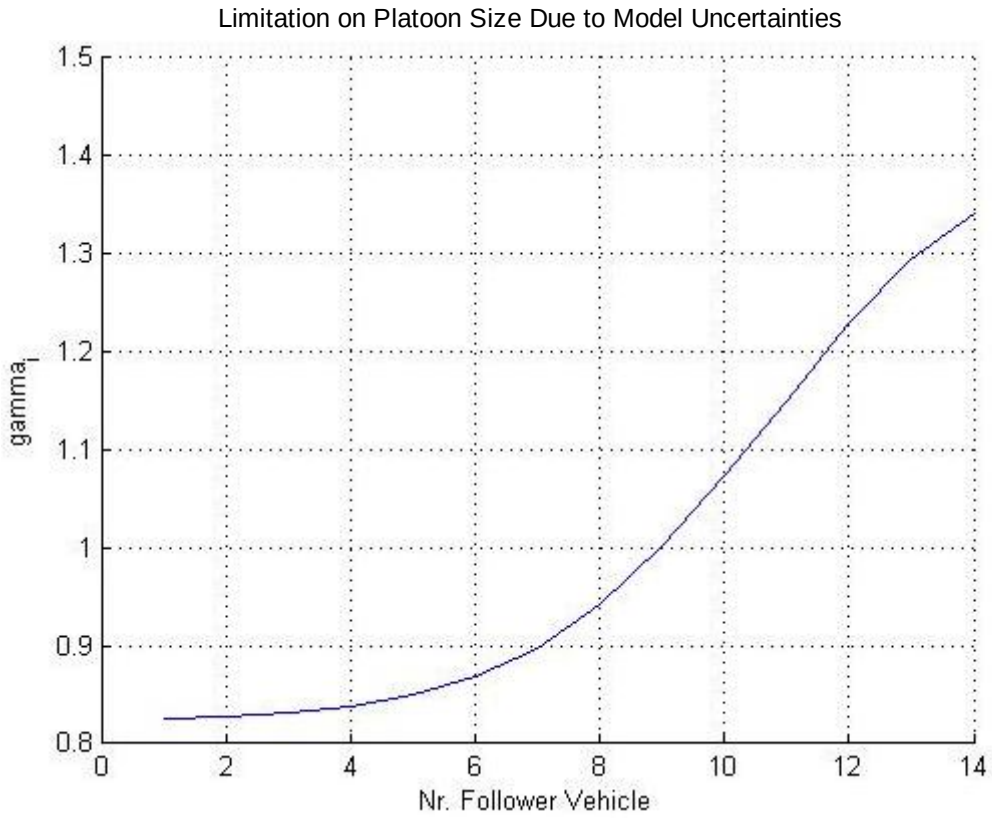

Figure 7.6.3.1: Limitation on platoon size due to model uncertainties.

It is clearly evident that string-stability can only be guaranteed up till the 8th vehicle. This is a rather conservative estimation. For more information, please refer to Patent I2828SE00.

8 Discussion and Conclusions

8.1 Controller Methods

From the results presented in the previous section, there are several interesting notes that can be made. For the PD-controller, it is seen that, for the tuning methods used, at the worst case no more than 40% overshoot occurs. If the aim in the design is to maintain a rise-time around 1 second, the overshoot would be approximately 20-25%, with a reasonable settling time, for the case of setting the crossover frequency to 2rad/s, while it is relatively lower for the case of the crossover being 1rad/s. This is mainly due to the fact that there is a variation in the rise-time chosen within the tolerance range as it is higher in the latter case. The least overshoots were achieved at high speeds and small look-ahead distances or at low speeds and large look-ahead distances. Thus it is possible to achieve relatively low overshoots in the desired operating ranges. To achieve the least overshoot, the requirement on the desired phase margin has to be set high, on the downside that the rise-time in the case where crossover is 1rad/s would be considerably higher than 1 and considerably lower in the other case. There is also the fact that having a higher phase margin results in a response with a slower settling time than in the normal settings of close to 60 degrees. This could be compensated for by choosing a higher crossover frequency, which would correspond to larger proportional action and subsequently larger overshoot.

Correspondingly, for the PDD-controller, by using the design in Section 5.2, the maximum overshoot is around 45%, and does not show any added value over the PD-controller, since the former presents less overshoot over more operating regions, especially the desired ones with high speeds and small look-ahead distances. However, the controller does not ask of as large control signals as the PD controller. Also, it can be seen that the control signals are slower than in the PD case, resulting in a slower rise-time. Thus, the less overshoot desired from the response of the system the more demand on a faster control signal there is. One advantage to using this method is that more phase may be added to the system, making it more resilient to delays that might appear.

The full pole-placement using additional derivatives presents difficulties when implementing, since the inclusion of the actuator will move them out of their positions. For velocities less than 10m/s, it was noted that either a non-minimum phase effect occurs or a dominating pair of complex conjugate zeros are introduced by the controller. These zeros would not move remarkably as poles were shifted, and thus this controller presents issues when working out of its range of operation. A suggestion would be to use a different tuning method for this area. However for the ranges the experiment was conducted in the responses were rather consistent. On the downside, the method lacks the simple and intuitive tuning offered by the PD- and PDD-controllers. In addition, the control signals required were larger than the other two cases, mainly because the resulting step-responses were larger.

In all cases it can be seen that overshoot cannot be avoided in the system, due to several reasons observed during various simulations. It was noted that a zero would be introduced by the controller that is always closer to the imaginary axis than the dominating pole also

introduced by the controller. The pair moves together and as overshoot decreases, they get closer and closer to each other until they cancel out at the origin when K_p goes to zero. This constitutes to having no proportional term in the controller. Another reason is that the dominating poles are complex and hence leading to an oscillatory response. In addition, having more than one zero in between the two dominating real poles leads to overshoot as well. Based on these observations, the nature of double integrator systems was investigated. Thus, an analytical proof of inherent overshoot in double integrator systems, when using the conventional controllers mentioned above, is given in Appendix A. The proof states that in order to avoid overshoot, the proportional gain of the controller should be set to zero. Using a purely derivative-acting controller would mean that solely the rate-of-change of the error is being corrected for. In a vehicle following application, there might be cases where a stationary error occurs, i.e. there is a lateral offset between the vehicles, but it is neither increasing nor decreasing, rendering the controller non-acting.

Furthermore, it can be seen that a fixed rise-time cannot be achieved under all operating condition for a fixed desired crossover frequency and desired phase margin. The same goes for achieving minimal overshoot. This is due to the plants dynamics, and thus there is no fixed setting method that would satisfy all demands under all operating regions.

8.2 String Stability

As mentioned in the results section, the proposed strategies 2, 3 and 4 do guarantee string stability for an infinite number of vehicles in a platoon assuming perfect knowledge of the vehicles parameters. It was also shown that topology 4 can guarantee string stability for a finite number of vehicles in a platoon when there are reasonable uncertainties in the parameters of the vehicles. Also, topologies 3 and 4, as a consequence of guaranteeing string stability, also include path following. Thus, it is a case where path following is integrated as a part of the regulation problem and has proven to perform very well in the lane change manoeuvre. However, more testing on real road profiles need to be done to validate the performance of the proposed topologies. For topologies 3 and 4, it was also noted that the maximum steering-wheel angle requested increases down the platoon and hence will possibly limit the number of vehicles in the platoon. In general, it is shown that string stability cannot be achieved without communication from preceding vehicles.

9 Future Work

This work was restricted to vehicles considered travelling at a constant velocity and with equal spacing between individuals in the platoon. Since the characteristics of the plant is heavily dependent on both velocity and look-ahead distance, controllers designed for specific parameters would be rendered useless or inconsistent in behaviour. If one of these parameters would vary during manoeuvres it would lead to the model considered turning nonlinear, and thus further analysis would be required.

Furthermore, as assumptions were made that parameters concerning the vehicle are predetermined and known, robustness tests and evaluations should be conducted to see the effect of parameter perturbations. Testing and validation in vehicles would provide a stronger basis to the claims and relations presented in this report.

In the case of working with controllers with high complexity, a complete analysis of conditions regulating the positioning of poles must be made. The inclusion of dynamics presented from the actuator will distort and move the poles from their desired positions. Taking the actuator into consideration would simplify the design process; however it will also place more requirements on the amount of signals measured (in this case, higher order derivatives), and in the case of unavailable information lead to sensitivity to noise since numerical differentiation is needed to be performed.

Since it is proven in Appendix A that it is impossible to achieve a over-damped response for double integrator systems using conventional methods, more focus should be put on finding more advanced control structures that would remove overshoot.

Proper tests have to be made to validate the accuracy of the vehicle model being used, as it will reflect on the string stability results.

10 References

[1] Rajamani, R. (2006) *Vehicle Dynamics and Control*. Ort: Publisher

[2] Vehicle Platooning and Automated Highways. *California Path Institute*. http://www.path.berkeley.edu/ (2011-06-13)

[3] Bergenhem, C. et al. (2010) Challenges of Platooning on Public Motorways. *17th World Congress on Intelligent Transport Systems*, October 25-29th, Busan, Korea.

[4] Özgüner, Ü. et al. (1995) An analytical study of vehicle steering control. *Proceedings of the 4th IEEE Conference on Control Applications* pp.125-130

[5] Sheikholeslam, S. and Desoer, C. (1991) Combined Longitudinal and Lateral Control of a Platoon of Vehicles: A System-level Study. *Path Technical Memorandum 91-3*

[6] Choi, J.Y. et al. (2002) Lateral Control of Autonomous Vehicle by Yaw Rate Feedback. *KSME International Journal* 16-3:pp.338-343

[7] Zak, S.H. (2009) An Introduction to Proportional-Integral-Derivative (PID) Controllers. Lecture notes, Purdue University.

[8] Åström, K.J. (2002) Control System Design. Department of Mechanical and Environmental Engineering, University of California, Santa Barbara.

[9] Dorf, R.C. and Bishop, R.H. Modern Control Systems. Prentice Hall, 2008 Upper Saddle River.

[10] Swaroop, D. and Hedrick, J.K. (1996) String Stability of Interconnected Systems. *IEEE Transaction on Automatic Control.* Vol. 41, No. 3.

[11] Cook, P.A. (2005) Conditions for String Stability. *Systems & Control Letters 54*. pp.991-998.

[12] Papadimitriou, I. and Tomizuka M. (2004) Lateral control of platoons of vehicles on highways: the autonomous following based approach. *Int. J. Vehicle Design* Vol. 36, No. 1

[13] Papadimitriou I. and Lu G., Tomizuka M. (2003) Autonomous Lateral Following Considerations for Vehicle Platoons. *Proceedings of the 2003 IEEE/ASME* (AIM 2003)

Appendix A

A.1 Proof of inherent overshoot in double integrator plants

It can be verified analytically that it in fact is not possible to avoid overshoot in a system consisting of a double integrator, using simple controllers.

Consider the plant

$$G(s) = \frac{1}{s^2} \tag{A.1.1}$$

and the PD-controller

$$C(s) = K_p + K_d s \tag{A.1.2}$$

The closed loop system would thus be

$$G_{closed}(s) = \frac{G(s)C(s)}{1+G(s)C(s)} = \frac{K_p+K_d s}{s^2+K_p+K_d s} \tag{A.1.3}$$

The step-response of this system can be written as

$$\frac{G_{closed}(s)}{s} = \frac{1}{s}\frac{K_p+K_d s}{s^2+K_p+K_d s} \tag{A.1.4}$$

Performing the replacement $s = j\omega$ yields

$$\frac{1}{j\omega}\frac{K_p+K_d j\omega}{-\omega^2+K_p+K_d j\omega} = \frac{K_p+K_d j\omega}{-j\omega^3+K_p j\omega-K_d\omega^2} \tag{A.1.5}$$

The magnitude of this function can be evaluated by separating the real and imaginary parts.

$$\left|\frac{G_{closed}(s)}{s}\right| = \frac{\sqrt{K_p^2+K_d^2\omega^2}}{\sqrt{K_d\omega^2+\left(K_p\omega-\omega^3\right)^2}} \tag{A.1.6}$$

Thus, the condition holds that equation (A.1.6) must, for all frequencies, be less than or equal to 1 in order to avoid overshoot.

$$K_p^2 + K_d^2\omega^2 \leq K_d\omega^2 + \left(K_p\omega - \omega^3\right)^2 \tag{A.1.7}$$

Reformulating the above equation, it is easily seen that the proportional gain is upper-bounded.

$$K_p^2 \leq K_d\omega^2 + \left(K_p\omega - \omega^3\right)^2 - K_d^2\omega^2 \tag{A.1.8}$$

At frequency $\omega = 0$, the following inequality must hold.

$$K_p^2 \leq 0 \tag{A.1.9}$$

Thus the only valid choice of proportional gain is 0, and the controller reduces to one with purely derivative action. The same result follows when using higher order derivative controllers.

In this application, this leads to the problem of only regulating the change-of-rate in the lateral deviation; thus if the vehicle has a stationary error, no corrections will be made.

A.2 Proof of inherent overshoot in general double integrator plants

The proof above can be expanded to the general case, where the plant is assumed to be

$$G(s) = \frac{A(s)}{s^2 B(s)} \tag{A.2.1}$$

Its frequency-domain equivalent can be divided into two parts; one containing the real components of the system and another containing the imaginary.

$$A(j\omega) = a(\omega) + jb(\omega) \tag{A.2.2}$$

$$B(j\omega) = c(\omega) + jd(\omega) \tag{A.2.3}$$

For the system to be of double integrator form, it is required that

$$a(0) \neq 0 \tag{A.2.4}$$

otherwise it would constitute to the numerator of equation (A.2.1) only consisting of terms involving the complex Laplace variable s, and would thus cancel out the integrator.

Furthermore,

$$b(0) = 0 \tag{A.2.5}$$

is required to hold, since, by definition, it contains the imaginary terms involving ω.

Thus, using the same controller as in the previous case, the closed-loop system can be written as

$$G_{closed}(j\omega) = \frac{\big(a(\omega)+jb(\omega)\big)\big(K_p+K_d s\big)}{-\omega^2\big(c(\omega)+jd(\omega)\big)+\big(a(\omega)+jb(\omega)\big)\big(K_p+K_d s\big)} \tag{A.2.6}$$

The magnitude of a step-response is

$$\left|\frac{G_{closed}(s)}{s}\right|_{s=j\omega} = \frac{\sqrt{\big(K_p a(\omega)-K_d b(\omega)\omega\big)^2+\big(K_d a(\omega)\omega+K_p b(\omega)\big)^2}}{\sqrt{\big(d(\omega)\omega^3-K_d a(\omega)\omega^2-K_p b(\omega)\omega\big)^2+\big(K_p a(\omega)\omega-c(\omega)\omega^3-K_d b(\omega)\omega^2\big)^2}} \tag{A.2.7}$$

Thus, the requirement is that

$$\big(K_p a(\omega) - K_d b(\omega)\omega\big)^2 + \big(K_d a(\omega)\omega + K_p b(\omega)\big)^2$$

$$\leq \big(d(\omega)\omega^3 - K_d a(\omega)\omega^2 - K_p b(\omega)\omega\big)^2)+\big(K_p a(\omega)\omega - c(\omega)\omega^3 - K_d b(\omega)\omega^2\big)^2 \tag{A.2.8}$$

Evaluating this function at $\omega = 0$ yields

$$K_p^2 a(0)^2 + K_p^2 b(0)^2 \leq 0 \qquad \text{(A.2.9)}$$

and it is proved that K_p must be zero in order to avoid overshoot, since $a(0)$ is non-zero by the condition (A.2.4), and $b(0)$ is by definition zero.